Research Square

Preprints are preliminary reports that have not undergone peer review.
They should not be considered conclusive, used to inform clinical practice,
or referenced by the media as validated information.

Sexual Dimorphism in Gene Expression: A Multi-Tissue Genome-Wide Study in BXD Mice and Potential Insights into Human Biology

Jiamin Ma
Harbin Medical University
Lishi Wang
Inner Mongolia Medical University
Gang Yuan
China Agricultural University
Chrishan Fernando
Purdue University West Lafayette
Lan Yao
University of Tennessee Health Science Center
Wei Dong
University of Tennessee Health Science Center
Cheng Tian
St. Jude Children's Research Hospital
Anna Bukiya
University of Tennessee Health Science Center
Monica Jablonski
University of Tennessee Health Science Center
Helin Feng
Fourth Hospital of Hebei Medical University
Daniel Li
University of Toronto
Lu Lu
University of Tennessee Health Science Center
Yan Jiao
University of Tennessee Health Science Center
Jiafu Ji
Peking University Cancer Hospital
Gang Wang
Harbin Medical University
Weikuan Gu
wgu@uthsc.edu

University of Tennessee Health Science Center

Research Article

Keywords: Sex Differences, Gene Expression, Genetic Correlation, Chromosomes, Tissues

Posted Date: June 19th, 2026

DOI: https://doi.org/10.21203/rs.3.rs-9936472/v1

License: This work is licensed under a Creative Commons Attribution 4.0 International License. Read Full License

Additional Declarations: No competing interests reported.

Abstract

Sex-biased gene expression contributes to physiological and disease differences between females and males. This study re-analyzed publicly available GeneNetwork expression datasets from BXD recombinant inbred mice across seven tissues, including adrenal gland, amygdala, hypothalamus, kidney, spleen, liver, and pituitary gland, to characterize tissue-dependent sex-biased expression and prioritize candidate regulatory loci. Because these datasets were generated using microarray platforms rather than RNA-seq, probe-level expression traits were analyzed and then mapped to genes. Male and female strain-level mean expression values were compared using paired two-tailed t-tests across matched BXD strains, followed by Bonferroni correction, and sex-biased probes were defined as $q < 0.05$. Functional enrichment, correlation-network analysis, eQTL mapping, and contextual comparison with human GTEx data were performed. Sex-biased expression was strongly tissue-dependent, with liver, adrenal gland, kidney, and pituitary showing larger proportions of sex-biased probes than amygdala, hypothalamus, and spleen. No autosomal gene was shared across all seven tissues, whereas X-linked genes showed more consistent sex-biased expression. Liver EDEGs were enriched for xenobiotic, steroid, bile-acid, and lipid-metabolic functions, while smaller DEG sets in amygdala, hypothalamus, and spleen were associated with neuronal signalling, reproductive regulation, heme metabolism, and immune response. Overall, this re-analysis supports strong tissue specificity in sex-biased expression in BXD mice and highlights candidate genes and regulatory loci for future experimental validation.

1 Introduction

Sex is a major biological variable influencing physiology, disease susceptibility, therapeutic response, and aging(Klein & Flanagan, 2016; Oliva et al., 2020). Although males and females share nearly identical genomes, substantial differences in gene expression contribute to sexually dimorphic traits across multiple organ systems(Ingleby et al., 2014; Klein & Flanagan, 2016; Lopes-Ramos et al., 2020; Oliva et al., 2020; Parsch & Ellegren, 2013). These differences influence diverse biological processes, including metabolism, immune responses, neurodevelopment, and endocrine regulation, and are associated with sex-biased prevalence and progression of many human diseases, including autoimmune disorders, cardiovascular disease, metabolic syndrome, and cancer(Klein & Flanagan, 2016; Ngo et al., 2014; Regitz-Zagrosek & Kararigas, 2017; Vera et al., 2023).

Comparative studies across species consistently demonstrate widespread sex-biased transcription. In humans, Genotype-Tissue Expression (GTEx) and related regulatory-network analyses have shown that sex affects both expression levels and gene-regulatory architecture across many tissues(Consortium et al., 2017; Gay et al., 2020; Khodursky et al., 2022; Lopes-Ramos et al., 2020; Mele et al., 2015). In mice, sex-biased expression has been particularly well studied in liver and kidney. In liver, prior work established extensive sex differences controlled by pituitary growth hormone secretion, STAT5-dependent transcription, strain background, and genetic variation(Conforto & Waxman, 2012; Gatti et al., 2007; Gatti et al., 2010; Lau-Corona et al., 2020; Waxman & O'Connor, 2006). In kidney, bulk, single-cell, spatial, and multi-omic studies have demonstrated substantial sex-biased expression, especially in proximal tubular compartments and during postnatal maturation(Chen et al., 2023; Chen et al., 2025; Ransick et al., 2019; Si et al., 2009). In addition, sex-biased expression patterns have been described in several brain regions and immune tissues, highlighting the widespread and tissue-dependent nature of sexual dimorphism(Khodursky et al., 2022; Lopes-Ramos et al., 2020; Mozhui et al., 2012). These studies provide an essential framework for interpreting any new analysis of sex-biased expression in these organs.

Despite substantial progress, several challenges remain. Many prior studies have focused on single tissues or single biological systems, making it difficult to compare sexually dimorphic expression patterns across organs within a unified genetic framework(Care et al., 2018; Voskuhl et al., 2018). Furthermore, the relative contributions of autosomal and sex chromosome-associated transcriptional programs across tissues remain incompletely understood(Mank, 2017). Comparative systems-level analyses integrating multiple tissues within the same genetically defined population may therefore provide additional insight into tissue-specific and shared mechanisms of sexual dimorphism(Khodursky et al., 2022; Lopes-Ramos et al., 2020).

The BXD recombinant inbred mouse family represents one of the most extensively characterized genetic reference populations for systems genetics studies(Cao et al., 2018; Crowley et al., 2015; Werner et al., 2017). Derived from crosses between C57BL/6J and DBA/2J strains, BXD mice provide a powerful resource for investigating complex genetic regulation of gene expression and phenotypic variation(Peirce et al., 2004). Publicly available GeneNetwork datasets generated from BXD strains include transcriptomic profiling across multiple tissues, enabling integrative cross-tissue analyses of sex-biased expression patterns(Mulligan et al., 2017).

In the present study, we performed a comparative re-analysis of publicly available GeneNetwork transcriptomic datasets from seven mouse tissues, including adrenal gland, amygdala, hypothalamus, pituitary gland, kidney, spleen, and liver. Using differential expression analysis, functional enrichment, network analysis, and expression quantitative trait locus (eQTL) mapping, we investigated tissue-specific and shared patterns of sexually dimorphic gene expression across autosomal and X-linked genes. We further compared selected mouse findings with human transcriptomic data to evaluate the conservation of sex-biased expression patterns across species. Our results provide a systems-level overview of tissue-dependent sexual dimorphism in gene expression and highlight potential regulatory pathways associated with sex-biased biological functions.

2 Results

Global landscape of sex-biased gene expression across mouse tissues

To investigate tissue-specific patterns of sexually dimorphic gene expression, we performed a comparative re-analysis of publicly available GeneNetwork transcriptomic datasets derived from seven mouse tissues, including adrenal gland, amygdala, hypothalamus, pituitary gland, kidney, spleen, and liver. Because these datasets were generated using different microarray platforms and sample compositions (Supplementary Table S1), differential expression analyses were performed independently within each tissue using sex-matched strain comparisons when available.

Across all tissues, 123,129 autosomal probes and 516 X-linked probes were analyzed. Sex-biased probes were defined by paired male-female comparison across matched BXD strain means with Bonferroni-adjusted q < 0.05. The number and proportion of DEGs varied substantially by tissue: amygdala, hypothalamus, and spleen contained relatively few sex-biased probes under this threshold, whereas liver, adrenal gland, kidney, and pituitary contained larger numbers (Table 1; Fig. 1A). We compared DEGs across tissues and observed that no autosomal gene was shared by all seven tissues. UpSet plot analysis was used to visualize common and unique genes among tissues (Fig. 1B). The most common DEG was *Greb1*, which was detected in the adrenal gland, amygdala, hypothalamus, kidney, and pituitary gland, making it the only gene shared by five tissues (Fig. 1C). Gene Ontology (GO) (Ashburner et al., 2000; Consortium et al., 2023)and Kyoto Encyclopedia of Genes and Genomes (KEGG) pathway enrichment analyses (Kanehisa et al., 2025) were performed separately for each tissue using only terms passing adjusted q < 0.05 (Supplementary Table S2). The spleen showed a distinct enrichment profile, whereas kidney and liver, and adrenal gland and pituitary gland, showed relatively greater similarity in enrichment patterns (Fig. 1D).

Table 1
Number and proportion of sex-biased probes with Bonferroni-adjusted q < 0.05 across chromosomes and tissues

n/N[a](%)	Adrenal	Amygdala	Hypothalamus	Kidney	Liver	Pituitary	Spleen
ChrX	129/1207(10.69)	10/1207(0.83)	12/1207(0.99)	133/1442(9.22)	92/691(13.31)	129/1207(10.69)	11/1271(0.87)
Chr1-19	3127/27031(11.57)	14/27031(0.05)	20/27031(0.07)	4022/42996(9.35)	2303/19511(11.80)	2787/28031(10.31)	62/28588(0.22
Chr1	174/1738(14.27)	1/1738(0.06)	2/1738(0.12)	239/2278(8.57)	149/1204(12.38)	259/1738(14.96)	7/1760(0.40)
Chr2	248/2274(10.91)	0/2274(0.00)	1/2274(0.04)	290/3592(8.07)	175/1779(9.84)	221/2274(9.72)	2/2334(0.09)
Chr3	163/1343(12.14)	1/1343(0.07)	1/1343(0.07)	255/2306(11.06)	125/965(12.95)	159/1343(11.84	4/1390(0.29)
Chr4	214/1753(12.21)	0/1753(0.00)	0/1753(0.00)	259/2715(9.54)	136/1219(11.16)	153/1753(8.73)	2/1810(0.11)
Chr5	224/1634(13.71)	0/1634(0.00)	0/1634(0.00)	237/2825(8.39)	147/1219(12.06)	182/1634(11.14)	7/1682(0.42)
Chr6	180/1520(11.84)	0/1520(0.00)	1/1520(0.07)	256/2501(10.24)	133/1167(11.40)	139/1520(9.14)	4/1553(0.26)
Chr7	180/2430(7.41)	1/2430(0.04)	2/2430(0.08)	245/3001(8.16)	125/1692(7.39)	167/2430(6.87)	0/2576(0.00)
Chr8	173/1382(12.52)	0/1382(0.00)	1/1382(0.07)	245/2214(9.72)	110/980(11.22)	132/1382(9.55)	1/1398(0.07)
Chr9	197/1595(12.35)	0/1595(0.00)	0/1595(0.00)	229/2403(9.53)	143/1171(12.21)	186/1595(11.66)	3/1607(0.19)
Chr10	169/1299(13.01)	0/1299(0.00)	4/1299(0.31)	219/2071(10.57)	105/907(11.58)	146/1299(11.24)	0/0321(0.00)
Chr11	227/2020(11.24)	1/2020(0.05)	0/2020(0.00)	271/3421(7.92)	176/1561(11.27)	186/2020(9.21)	6/2053(0.29)
Chr12	145/995(14.57)	2/995(0.20)	2/995(0.20)	144/1699(8.48)	87/687(12.66)	119/995(11.96)	2/2019(0.20)
Chr13	127/1076(11.80)	2/1076(0.19)	1/1076(0.09)	196/1799(10.89)	95/730(13.01)	108/1076(10.04)	4/1107(0.36)
Chr14	109/1122(11.59)	1/1122(0.09)	0/1122(0.00)	149/1648(9.04)	95/707(13.44)	105/1122(9.36)	6/1175(0.51)
Chr15	127/1061(1.97)	1/1061(0.09)	1/1061(0.09)	195/1770(11.02)	121/755(16.03)	137/1061(12.91)	3/1967(0.15)
Chr16	110/904(12.17)	1/904(0.11)	0/904(0.00)	160/1539(10.40)	83/666(12.46)	104/904(11.50)	3/907(0.33)
Chr17	132/1305(10.11)	0/1305(0.00)	2/1305(0.15)	191/1924(9.93)	127/916(13.86)	103/1305(7.89)	3/1323(0.23)
Chr18	98/673(14.56)	2/673(0.30)	2/673(0.30)	123/1271(9.68)	49/501(9.78)	83/673(12.33)	3/692(0.43)
Chr19	130/907(14.33)	1/907(0.11)	0/907(0.00)	150/1520(9.87)	122/685(17.81)	98/907(10.80)	2/914(0.22)

Note: N-the total number of probes; n-the number of probes which the gene expression's q-value (Bonferroni adjust p-value) < 0.05.

We further analyzed X-linked DEGs across the seven tissues (Fig. 1E). *Kdm6a*, *Eif2s3x*, and *Xist* were consistently detected as sex-biased across all seven tissues. Functional enrichment analysis of these X-linked DEGs revealed similar GO terms in the amygdala and hypothalamus, which also showed closer functional relationships to the spleen than to endocrine tissues (Fig. 1F; Supplementary Tables S3).

Despite being shared across tissues, the protein products of these DEGs exhibited low sequence similarity, with a maximum amino acid identity of 11.7% and similarity of 28.9% (Fig. 1G)—both below the 40% threshold typically required to infer functional similarity(Pearson, 2013).

To focus subsequent analyses on the most robust sex-biased signals, we further defined a subset of extremely differentially expressed genes (EDEGs). EDEGs were selected from Bonferroni-significant DEGs with extremely small p-values, representing high-confidence sex-biased genes within each tissue. These EDEGs were highly tissue-specific. Among autosomal genes, *Akr1d1* and *Akr1c18* were identified in the adrenal gland; *Slc7a12*, *Cyp7b1*, *Slc7a13*, *Slco1a1*, and *Acsm3* were identified in the kidney; and *Rxfp1* was identified in the pituitary gland. The liver contained the largest EDEG set, with 121 identifiable genes (Supplementary Table S4). Among X-linked EDEGs, recurrent sex-biased genes included *Xist*, *Kdm6a*, *Kdm5c*, *Eif2s3x*, and *Ddx3x* (Supplementary Table S5). These high-confidence genes were prioritized for subsequent tissue-specific analyses.

Research of EDEGs on autosomal chromosomes across tissues

Akr1d1 is the most different expressed genes between male and female in adrenal glands

In the adrenal gland, *Akr1d1* and *Akr1c18* were identified EDEGs. As *Akr1c18* is absent in humans, subsequent analyses focused on *Akr1d1*. Significant sex differences in *Akr1d1* expression were observed in the adrenal gland, liver, and kidney, with the largest expression difference detected in the adrenal gland (Fig. 2A). To investigate tissue relationships of *Akr1d1* expression, Pearson correlation analyses were performed across the seven examined tissues. *Akr1d1* expression in kidney showed relatively strong positive correlations with expression in liver and adrenal gland datasets in both male and female mice (Fig. 2B) regulatory differences within this tissue.

Phenotype and gene correlation analyses identified sex-dependent association patterns for *Akr1d1* in adrenal gland datasets (Fig. 2C). In male mice, weight loss-related phenotypes showed strong positive correlations (r = 0.890) with *Akr1d1* expression, whereas in female mice sibling sucking-associated phenotypes demonstrated strong negative correlations (r = − 0.948). The genes most strongly correlated with *Akr1d1* expression were *Atp8b1* in male mice (r = 0.843) and *Cyp21a1* in female mice (r = 0.947). However, only limited correlations were observed between these associated genes, indicating that the transcriptional relationships surrounding *Akr1d1* differ substantially between sexes.

Expression quantitative trait locus (eQTL) analyses were subsequently performed to investigate potential genetic regulation of *Akr1d1* expression (Fig. 2D). In female mice, suggestive distal eQTL signals were identified on chromosome 17 for adrenal gland, chromosome 14 for kidney, and chromosome 7 for pituitary gland datasets (Supplementary Figure S1). In male mice, both local and distal suggestive eQTL signals were observed, including loci on chromosomes 6 and 9. Candidate regions associated with these eQTL peaks contained multiple SNPs and annotated genetic elements (Supplementary Tables S6–S10).

Among these candidate loci, SNP rs32328305 within the *Herc2* locus was located near the peak LRS region in female pituitary gland datasets (Supplementary Figure S1A, S1C). This SNP represents a T-to-G substitution within an intronic region differing between B6 (T) and D2 (G) strains. Comparison of *Akr1d1* expression between genotypes demonstrated a significant association only in the female pituitary gland dataset (p = 0.0002) (Fig. 2E), suggesting a potential relationship between the *Herc2* locus and *Akr1d1* expression in this tissue(Wang et al., 2014).

To further evaluate potential functional relationships, correlation networks involving *Akr1d1*, *Herc2*, and their top-associated genes and phenotypes were examined (Fig. 2F). Although several indirect associations were identified, no strong direct correlation between *Akr1d1* and *Herc2* expression was observed, indicating that additional experimental studies will be required to clarify potential regulatory interactions.

2.2.2 Kidney sex-biased genes exhibit coordinated correlation and regulatory patterns

In the kidney, five sex-biased DEGs were identified: *Slc7a12* and *Cyp7b1* on chromosome 3, *Slc7a13* on chromosome 4, *Slco1a1* on chromosome 6, and *Acsm3* on chromosome 7. Correlation analyses revealed substantial overlap among their top-associated genes and phenotypes, suggesting partially coordinated transcriptional and phenotypic relationships (Table 2, Fig. 3A). As *Slc7a12* does not have a clear human ortholog, subsequent analyses focused primarily on *Cyp7b1*, *Slc7a13*, *Slco1a1* and *Acsm3* (*Sah*).

Table 2
Top-associated genes and phenotypes of kidney sex-biased EDEGs

DEGS	TOP GENES	TOP PHENOTYPES
Slco1a1 M	Slco1a1 (last 3 exons)	Liver copper level
Slco1a1 F	Ddx3y	Ethanol Response
Slc7a13 M	Xist	Anti IgG2b level
Slc7a13 F	Slco1a1	Ethanol response
Cyp7b1 M	Cyp7b1(exon 5)	Anti IgG2b level
Cyp7b1 F	Cyp7b1(exon 5)	Ethanol response
Slc7a12 M	Sucnr1	OTU199 metabolism
Slc7a12 F	Eif2s3y	Large Unknown Cells
Sah M	Slco1a1	Y-maze test
Sah F	Uty	Ethanol Response

Expression profiles of these genes across seven tissues are summarized in Fig. 3B. Among them, *Cyp7b1* exhibited sex-biased expression not only in kidney, but also in liver, adrenal gland, and pituitary gland datasets. *Slc7a13* and *Slco1a1* additionally showed sex-biased expression in liver and adrenal gland datasets, whereas *Acsm3* demonstrated predominant liver-associated sex bias. These findings suggest that several kidney-associated EDEGs may participate in broader tissue-dependent metabolic or endocrine transcriptional programs.

Correlation network analyses were subsequently performed to evaluate relationships among the top-associated genes and phenotypes linked to these kidney EDEGs across tissues (Supplementary Figure S2A). Several tissue- and sex-dependent association patterns were observed. In female mice, phenotypes positively correlated with multiple kidney EDEGs were frequently associated with ethanol-response traits. In contrast, correlations involving ethanol-response phenotypes in male mice varied substantially across tissues and genes. Additional phenotype associations included anti-IgG2b-related immune traits, which showed opposite directional correlations depending on tissue and sex context.

Gene–gene correlation analyses further demonstrated partial connectivity among kidney EDEGs. *Slco1a1* exhibited strong self-associated correlations and was additionally correlated with *Slc7a13* in female mice and *Acsm3* in male mice. Several associations involving X chromosome-linked genes were also observed. For example, *Xist* demonstrated a strong negative correlation with *Slc7a13* in male kidney datasets but showed positive correlations in hypothalamus-associated analyses. Overall, these findings indicate that sex-biased kidney EDEGs participate in complex tissue-specific transcriptional and phenotypic association networks.

To investigate potential genetic regulation of these kidney-associated EDEGs, eQTL analyses were performed across multiple tissues (Supplementary Figure S2B; Supplementary Tables S11-S22). After the genotype-expression comparisons between B6 and D2 alleles demonstration, a total of 12 SNPs and 10 candidate regulatory genes were identified in human orthologs (Table 3). Network analyses integrating kidney EDEGs with their candidate-associated genes and phenotypes revealed several tissue- and sex-dependent relationships (Fig. 3C). For example, *Cyp7b1* showed negative correlations with the top-related phenotype of Plcb4 (liver lipidomics), while the ethanol-response phenotype associated with *Cyp7b1* also negatively correlated with the top-related phenotype of *Hao1* (midbrain dopamine levels). Analyses involving *Slc7a13* and *Masp1* demonstrated indirect associations between candidate-associated genes and lipid-related phenotypes. In contrast, only limited correlations were observed among *Slco1a1*, *Timm21*, and *Fbxo15* in male pituitary gland datasets. For *Acsm3*, network analyses identified associations with multiple candidate genes, including *Mosmo*, *Acsm1*, *Acsm5*, *Slc12a6*, and *Emc7*. Several correlations involved metabolic, immune, and neurobehavioral phenotypes, further supporting the tissue-specific complexity of kidney-associated sex-biased transcriptional networks. However, because these findings are based on correlation and eQTL analyses derived from public datasets, additional experimental validation will be required to determine direct regulatory mechanisms.

Table 3
SNPs and candidate-associated genes identified from eQTL intervals

Source Genes	Tissue	SNPs	Alleles (B6/D2)	Most Severe Consequence	Candidate Genes	Candidate Gene's Location	
						Female	Male
Cyp7b1	Kidney female	rs13476784	C/A	Intron variant	Hao1	Kidney, Liver	Hypothalamus
		rs27252871	T/C	Intron variant	Plcb4	Kidney, Liver	Hypothalamus
		rs29523263	C/T	Intron variant			
		rs29716787	C/G	Intron variant			
Slc7a13	Pituitary male	rs4165334	T/C	Intron variant	Masp1		Pituitary, Liver
Slco1a1	Spleen male	rs29882288	G/A	3 prime UTR variant	Fbxo15		Pituitary
					Timm21		
Sah	Kidney female	rs6322316	T/C	Intron variant	Mosmo	Pituitary, Kidney	Liver, Hypothalamus, Spleen, Kidney
	Hypothalamus female	rs52710187	G/T	Intron variant	Slc12a6	Spleen, Hypothalamus	Hypothalamus
		rs3681694	T/C	Intron variant			
	Liver male	rs27506268	G/A	Intron variant	Emc7	Spleen, Hypothalamus	Kidney, Hypothalamus
		rs31513472	T/C	Intron variant	Acsm5	Pituitary, Kidney	Liver, Hypothalamus Spleen, Kidney
		D7Mit330	NA	Na	Acsm1	Pituitary, Kidney	Liver, Hypothalamus, Spleen, Kidney

2.2.3 Rxfp1 differentially expressed and associated with genome expression in between sexes in Pituitary gland

Rxfp1 was the only autosomal EDEG identified in the pituitary gland dataset. Significant sex-biased expression of *Rxfp1* was also observed in kidney and adrenal gland datasets, although the strongest difference was detected in the pituitary gland (Fig. 4A). To explore whether *Rxfp1* expression was associated with other genes or phenotypes in the GeneNetwork resource, we performed correlation analyses separately by sex. In female mice, *Reln* was the top correlated gene, and bone trait 38 was the strongest associated phenotype (Fig. 4B). Cross-tissue correlation analyses showed that Rxfp1-associated relationships varied across tissues and between sexes, suggesting that the transcriptional context of *Rxfp1* is tissue dependent (Fig. 4C).

We next performed eQTL analysis to identify potential genetic loci associated with *Rxfp1* expression. No significant eQTL was detected for *Rxfp1* in the pituitary gland dataset. However, a suggestive eQTL was identified on chromosome 15 in the female spleen dataset (Fig. 4D). This region included three candidate-associated genes, *Krt90*, *Espl1*, and *Aaas* (Supplementary Tables S23-S24). Because *Krt90* lacks a clear human ortholog, subsequent analyses focused on *Espl1* and *Aaas*.

Genotype-expression analysis showed that *Rxfp1* expression differed significantly between B6- and D2-associated alleles at the Aaas-associated locus in the female spleen dataset (Fig. 4E), suggesting that this locus may be associated with variation in *Rxfp1* expression. However, network analysis did not identify a strong direct correlation between *Rxfp1* and *Aaas* expression (Fig. 4F).

2.2.4 Liver shows extensive sex-biased gene expression linked to metabolic functions

Among the seven tissues analyzed, the liver contained the largest autosomal EDEG set. A total of 121 identifiable liver EDEGs were detected, with most showing higher expression in male mice (Fig. 5A). This broad hepatic sex-biased expression pattern is consistent with previously established sexual

dimorphism in liver metabolism and xenobiotic processing(Gatti et al., 2010).

Functional enrichment analysis of liver EDEGs revealed prominent enrichment of metabolic and detoxification-related pathways (Fig. 5B-5C). Male-biased genes were enriched for G protein–coupled receptor activity and olfactory receptor-related signaling, whereas female-biased genes were enriched for arachidonic acid metabolism, steroid hydroxylase activity, oxidation–reduction processes, chemical carcinogenesis, and cytochrome P450-related pathways (Fig. 5D-5E). These findings indicate that sex-biased hepatic transcriptional programs are strongly associated with metabolic and xenobiotic functions.

Protein–protein interaction analysis further identified functionally related modules among liver EDEGs (Fig. 5F). Female-biased genes included several metabolic and detoxification-related enzymes, such as *Fmo3*, *Hao3*, *Sult2a2*, *Cbr1*, *Gstt3*, and members of the Cyp2b family(Islami et al., 2021; Oliveira PA, 2007; Sun et al., 2013). Male-biased genes included signaling- and receptor-associated genes such as *Fgf6*, *Itga1*, *Lama3*, *Mindy3*, *Casp14*, *Mrgpre*, *Mc1r*, *Lgr8*, and *F2r*. These results suggest that hepatic sex-biased genes are organized into distinct functional groups related to metabolism, detoxification, and signaling regulation(Giretti & Simoncini, 2008; Valentino et al., 2013).

To evaluate potential cross-species relevance, liver EDEGs were compared with human liver expression datasets. Among the mouse liver EDEGs, 70 had identifiable human orthologs or corresponding expressed genes (Fig. 5A, Supplementary Table S25). Network analysis of these human-relevant genes identified modules involving the striatin family and fibroblast growth factor signaling components, including *Strn*, *Strn4*, *Fgfr2*, *Fgf6*, *Frs3*, and *Trim24* (Fig. 5G). Functional annotation of these human-relevant genes identified modules involving striatin family genes, fibroblast growth factor signaling components, PI3K–Akt signaling, lysosomal function, and positive regulation of biological processes (Fig. 5H–J, Supplementary Table S26).

Tissue-specific autosomal DEGs in amygdala, hypothalamus, and spleen.

Compared with liver, adrenal gland, kidney, and pituitary gland datasets, fewer autosomal DEGs were identified in the amygdala, hypothalamus, and spleen under the statistical thresholds used in this study. Although the number of DEGs was limited, functional enrichment analyses suggested tissue-specific biological patterns (Fig. 6).

In the amygdala dataset, 14 autosomal DEGs were identified, including four tissue-specific DEGs: *Gm9568*, *Gm5458*, *Pcdhb6*, and *Slc6a3* (Fig. 6A). Protein–protein interaction analysis did not reveal a strongly connected interaction module. However, GO and KEGG enrichment analyses indicated that these genes were associated with ion binding, transporter activity, receptor activity, channel activity, and positive regulation of potassium ion transport (Fig. 6B). These findings suggest that sex-biased autosomal genes in the amygdala may be related to neuronal signalling and ion transport processes.

In the hypothalamus dataset, 20 autosomal DEGs were identified. Functional enrichment analysis highlighted terms related to hormone signalling, nuclear receptor activity, ligand-activated transcription factor activity, synaptic organization, reproductive regulation, and mammary gland development (Fig. 6C–D). Several DEGs, including *Oxtr*, *Esr1*, *Crim1*, and *Tac2*, were associated with reproductive and endocrine-related biological processes. These results are consistent with the known role of the hypothalamus in neuroendocrine regulation and reproductive physiology.

In the spleen dataset, 62 autosomal DEGs were identified. Network analysis identified three main clusters associated with heme metabolism, mitochondrial iron transport, heme biosynthesis, chemokine-mediated signalling, and adaptive immune responses (Fig. 6E). Cluster-level expression patterns differed between sexes, with some immune- and heme-related clusters showing higher expression in females and others showing higher expression in males (Fig. 6F). These findings suggest that spleen autosomal DEGs may reflect sex-biased regulation of immune and hematopoietic-related functions(Handelsman et al., 2018; Sabino & Petroianu, 2021; Tamura, 1926).

X-linked DEGs show recurrent sex-biased expression across tissues

Because X chromosome-associated genes showed recurrent sex-biased expression across multiple tissues in the global analysis, we further examined high-confidence X-linked EDEGs in detail. Compared with autosomal EDEGs, which were largely tissue-specific, several X-linked EDEGs were detected repeatedly across tissues, including *Xist*, *Kdm6a*, *Kdm5c*, *Eif2s3x*, and *Ddx3x* (Supplementary Table S5; Fig. 1E).

Among these genes, *Xist* showed consistently higher expression in female mice across all seven tissues, consistent with its established role in X-chromosome inactivation (Fig. 7A). Other recurrent X-linked EDEGs, including *Kdm6a*, *Kdm5c*, *Eif2s3x*, and *Ddx3x*, were also differentially expressed in multiple tissues, although their expression patterns varied by tissue.

Functional annotation and network analysis of recurrent X-linked EDEGs suggested enrichment for genes involved in transcriptional regulation, chromatin modification, translation, and RNA metabolism (Fig. 7B). These functional categories differed from many autosomal EDEGs, which were more frequently associated with tissue-specific metabolic and transport-related pathways. This distinction supports the observation that X-linked and autosomal sex-biased genes may contribute to sexual dimorphism through partially different biological processes.

To explore potential genetic regulation of recurrent X-linked EDEGs, eQTL analyses were performed for selected genes. Detectable eQTL signals were mainly observed for *Kdm5c*. In female mice, *Kdm5c*-associated eQTLs were identified in liver and hypothalamus datasets, whereas in male mice an eQTL signal was detected in the hypothalamus dataset (Fig. 7C). Integration of eQTL mapping and interval analysis identified *Sema3e*, *Pclo*, and *Kcnd3* as candidate-associated genes for *Kdm5c*.

Genotype-expression comparisons suggested that *Sema3e* was associated with *Kdm5c* expression in the female pituitary gland dataset, whereas *Sema3e* and *Pclo* were associated with *Kdm5c* expression in the male amygdala dataset (Fig. 7D). Correlation analyses among *Kdm5c*, candidate-associated genes, and selected GeneNetwork phenotypes identified several indirect associations, including traits related to learning and memory, cocaine response, and MPTP response (Fig. 7E). However, these results should be interpreted as exploratory associations rather than evidence of direct regulatory interactions.

Overall, recurrent X-linked EDEGs showed broader cross-tissue recurrence than autosomal EDEGs, while still displaying tissue- and sex-dependent regulatory patterns. These findings suggest that X-linked sex-biased genes may contribute to shared regulatory features of sexual dimorphism across tissues, whereas autosomal sex-biased genes appear to be more strongly tissue-specific.

3 Methods

Public transcriptomic datasets

Publicly available transcriptomic datasets from BXD recombinant inbred mouse strains were obtained from the GeneNetwork platform. Seven tissues were analysed: adrenal gland, amygdala, hypothalamus, kidney, liver, pituitary gland, and spleen. Detailed dataset information, including tissue source, microarray platform, strain composition, sex balance, and preprocessing procedures, is summarized in Supplementary Table S1.

These datasets were generated previously by multiple independent laboratories. Most datasets were produced using Affymetrix Mouse Gene 1.0 ST exon-style microarrays, whereas the liver dataset was generated using Agilent two-color microarrays. Because the present study represents a secondary re-analysis of public datasets, sample preparation procedures, animal ages, pooling strategies, and sex balance differed among tissues.

Gene expression data processing

Probe-level expression data were obtained from GeneNetwork-derived expression tables. For Affymetrix datasets, expression values had been processed using Robust Multi-array Average normalization followed by log2 transformation and GeneNetwork scaling. For the Agilent liver dataset, expression values were generated using LOWESS normalization followed by log2 transformation. The normalized expression values provided by GeneNetwork were used for downstream analyses.

Because these datasets were generated using microarray platforms rather than RNA-sequencing technologies, expression traits were analyzed at the probe level and subsequently mapped to gene symbols for overlap analysis, functional annotation, and cross-species comparison.

Differential expression analysis

For each tissue, sex-biased expression was assessed by comparing female and male expression values for each probe. Sex-specific mean expression values and standard deviations were calculated for each probe, and differential expression between sexes was evaluated using a two-tailed Welch's t-test. The t statistic was calculated from the difference between female and male mean expression values divided by the standard error estimated from the two sex-specific variances. Degrees of freedom were estimated using the Welch–Satterthwaite approximation.

Raw p-values were adjusted for multiple testing using Bonferroni correction. Probes with Bonferroni-adjusted q-values < 0.05 were defined as sex-biased differentially expressed probes. Significant probes were then mapped to gene symbols and referred to as differentially expressed genes (DEGs) for downstream analyses.

Definition of extremely differentially expressed genes

To prioritize the most robust sex-biased signals, a subset of extremely differentially expressed genes (EDEGs) was defined. EDEGs were selected from Bonferroni-significant DEGs with extremely small p-values within each tissue. These high-confidence genes/probes were used for tissue-specific analyses, eQTL mapping, candidate-locus evaluation, and cross-species comparison.

Cross-tissue and chromosomal comparison

Sex-biased DEGs were compared across tissues separately for autosomal chromosomes and the X chromosome. The number and proportion of DEGs were calculated for each chromosome and tissue. Shared and tissue-specific DEGs were visualized using UpSet plots and summary plots. X-linked DEGs were analyzed separately to identify recurrent sex-biased genes across tissues.

Functional enrichment and network analysis

Gene Ontology and Kyoto Encyclopedia of Genes and Genomes enrichment analyses were performed for tissue-specific DEG and EDEG sets. Enrichment analyses were conducted using STRING and DAVID v6.8(Sherman et al., 2022). Enriched terms were considered statistically significant if they contained at least three genes and had an adjusted p-value, or q-value, < 0.05.

Protein–protein interaction networks were generated using STRING. STRING network analysis was restricted to protein–protein interactions with a minimum required interaction score of 0.4, corresponding to medium confidence. Network visualization and clustering were performed using Cytoscape when appropriate.

Gene–gene and gene–phenotype correlation analysis

Gene–gene and gene–phenotype correlations were explored using GeneNetwork tools. Matrix comparisons were performed using the Matrix function in GeneNetwork, and correlation networks were constructed using the Graph function. Pearson correlation coefficients were calculated to evaluate linear associations between normalized expression traits and available GeneNetwork phenotypes.

For selected EDEGs, the top correlated genes and phenotypes were identified separately by sex and tissue. Correlation strength was categorized descriptively as follows: strong negative correlation, − 1.0 to − 0.7; moderate negative correlation, − 0.7 to − 0.5; slight negative correlation, − 0.5 to 0; slight positive correlation, 0 to 0.5; moderate positive correlation, 0.5 to 0.7; and strong positive correlation, 0.7 to 1.0. These categories were used only to annotate network figures and should not be interpreted as evidence of causality.

For selected genes, the top 100 correlated phenotypes and top 100 correlated genes were compiled from GeneNetwork. Functional relevance of selected gene–phenotype and gene–gene associations was assessed by literature review using PubMed. Matched publications were reviewed by at least two investigators.

eQTL mapping and candidate-associated loci

Expression quantitative trait locus analysis was performed using GeneNetwork mapping tools for selected high-confidence EDEGs. Analyses were conducted separately by sex and tissue where applicable. Loci exceeding GeneNetwork suggestive or significant likelihood ratio statistic thresholds were further examined.

Candidate-associated genomic regions were evaluated using GeneNetwork Interval Analyst and Haplotype Analyst tools. SNP information was obtained from Ensembl(Cunningham et al., 2022), and candidate gene annotation was supplemented using GeneCards (Safran et al., 2010)and UniProt(Consortium, 2024). Candidate gene identification followed previously established protocols(Wang et al., 2014). Protein–protein interaction networks for candidate-associated genes were analyzed using STRING(Szklarczyk et al., 2023).

Candidate-associated genes were prioritized based on their location within eQTL intervals, B6/D2 allele differences, SNP annotation, and genotype-expression comparisons. These loci were interpreted as candidate-associated regions rather than confirmed regulatory genes.

Human comparison

Human transcriptomic data were used for contextual cross-species comparison. Mouse EDEGs were mapped to human orthologs or corresponding expressed genes where available. Human expression patterns were then examined to evaluate whether selected mouse sex-biased genes showed similar or divergent sex-biased expression trends in human tissues. Human data were not used for discovery analysis.

Software and statistical analysis

Statistical analyses and visualizations were performed using R. Plots were generated using packages including ggplot2, igraph, and ggraph. Network analyses were performed using STRING and Cytoscape. Unless otherwise specified, p-values were adjusted using Bonferroni correction, and q-values < 0.05 were considered statistically significant. P-values displayed as zero by software output were reported as threshold values, such as $p < 0.001$, rather than $p = 0.00$.

Comparison of amino acid composition.

Amino acid sequences of proteins encoded by the genes of interest were uploaded in FASTA format from the National Library of Medicine protein database (https://www.ncbi.nlm.nih.gov/protein)("Database resources of the National Center for Biotechnology Information," 2016). The sequences were aligned using the built-in alignment functions of Molecular Operating Environment (MOE) software (Chemical Computing Group, Montreal, Quebec, Canada). Identity and similarity metrics were computed to visualize amino acid sequence comparisons.

Ethical approval

declarations: Ethics approval is not applicable

4 Discussion

Overview of tissue-dependent sex-biased expression

This study re-analyzed public GeneNetwork microarray datasets to compare sex-biased expression across seven BXD mouse tissues. Overall, the results support a strongly tissue-dependent pattern of sexual dimorphism in gene expression. Liver and endocrine-associated tissues showed larger numbers of sex-biased probes under the thresholds used, whereas amygdala, hypothalamus, and spleen showed smaller autosomal DEG sets. These differences likely reflect both biological tissue specificity and technical factors, including microarray platform, probe coverage, sample composition, and filtering criteria, as summarized in Supplementary Table S1.

Functional enrichment networks further supported distinct patterns between autosomal and X-linked sex-biased genes. Autosomal DEG enrichment was more tissue-specific, with greater similarity between kidney and liver and between adrenal gland and pituitary gland, consistent with shared metabolic and endocrine functions (Fig. 1D). In contrast, X-linked DEG enrichment showed more recurrent functional themes across tissues, particularly among amygdala, hypothalamus, and spleen (Fig. 1F). These findings suggest that autosomal sex-biased genes may primarily reflect tissue-specific physiological programs, whereas recurrent X-linked genes may contribute to broader regulatory processes such as dosage compensation, chromatin regulation, translation, and RNA metabolism. However, enrichment overlap reflects annotation similarity rather than direct mechanistic regulation and should therefore be interpreted cautiously.

Autosomal EDEGs and tissue-specific biological functions

Autosomal EDEGs were largely tissue specific. In adrenal gland, Akr1d1 showed strong sex-biased expression and was associated with candidate eQTL signals, including a potential association with the *Herc2* locus. Because *Akr1d1* participates in steroid hormone and bile acid metabolism, its adrenal and metabolic-tissue expression pattern is consistent with endocrine regulation of sex-biased metabolism(Barnard et al., 2020; Colvin PL Jr, 1998; Nikolaou et al., 2019; Phelps et al., 2019; Rich et al., 2018).

In the kidney dataset, four high-confidence EDEGs with human relevance—*Cyp7b1*, *Slc7a13*, *Slco1a1*, and *Acsm3*—were associated with metabolic, transport, and immune-related phenotypes. *Cyp7b1* is involved in bile acid and steroid metabolism, *Slc7a13* in amino acid transport, *Slco1a1* in organic anion transport, and *Acsm3* in fatty acid metabolism(Iwai N, 2002; Matsuo et al., 2002; Phelps et al., 2019; Stiles et al., 2009; Thakkar et al., 2017; Vessey DA, 1999; Yahyaoui & Perez-Frias, 2019).The kidney results in the present study likely reflect differences in microarray platform, sample composition, and stringent filtering thresholds. Candidate-associated genes identified by eQTL and genotype-expression analyses, including *Hao1*, *Plcb4*, *Masp1*, *Fbxo15*, *Timm21*, *Mosmo*, *Acsm5*, and *Acsm1*, should therefore be considered exploratory and require experimental validation.

Although fewer DEGs were found in the amygdala, hypothalamus, and spleen, enrichment analyses still revealed biologically relevant patterns. Amygdala DEGs were linked to ion transport and neuronal signaling(Li et al., 2024), hypothalamic DEGs were associated with reproductive and lactational functions(Dale, 2020), and spleen DEGs showed cluster-level enrichment related to heme metabolism and immune response(Gal-Oz et al., 2019; Krumsiek et al., 2015). These findings suggest that even small DEG sets may reflect tissue-relevant sex-biased biological processes.

Liver EDEGs and sex-biased metabolic and signaling pathways

The liver showed the broadest sex-biased expression profile among the seven tissues analyzed, consistent with previous studies demonstrating extensive sexual dimorphism in hepatic metabolism, xenobiotic processing, and endocrine regulation(Conforto & Waxman, 2012; Gatti et al., 2007; Gatti et al., 2010; Lau-Corona et al., 2020; Waxman & O'Connor, 2006). Liver EDEGs were enriched in metabolic, detoxification, signaling, and lysosomal pathways. Female-biased EDEGs included *Fmo3*, *Hao3*, *Sult2a2*, *Cbr1*, *Gstt3*, and members of the Cyp2b family, which are associated with oxidation-reduction reactions, steroid metabolism, and xenobiotic processing(Islami et al., 2021; Oliveira PA, 2007; Sun et al., 2013). Male-biased EDEGs included receptor-, signaling-, and extracellular matrix-associated genes such as *Fgf6*, *Itga1*, *Lama3*, *Mindy3*, *Casp14*, *Mrgpre*, *Mc1r*, *Lgr8*, and *F2r(*Giretti & Simoncini, 2008; Valentino et al., 2013; van der Linden et al., 2018).

Among the human-relevant liver EDEGs, several genes mapped to functional modules with potential disease relevance. Two male-biased genes, *Strn* and *Strn4*, belonged to the striatin family (Fig. 6H). Striatins are scaffolding proteins involved in intracellular signalling and calcium–calmodulin-associated pathways, and previous studies have also linked them to steroid receptor signalling, including mineralocorticoid receptor and estrogen receptor pathways(Benoist et al., 2006; Garza et al., 2015; Gupta et al., 2017; Ruhs et al., 2017).

Another module involved fibroblast growth factor signaling components, including Fgf6, Frs3, Fgfr2, and Trim24. In this module, Fgf6 and Frs3 showed higher expression in males, whereas Trim24 showed lower expression in males. Because FGF signaling participates in development, tissue repair, MAPK pathway activation, and tumor-related biological processes, this module may represent a sex-biased signaling network relevant to liver physiology(Appikonda et al., 2016; Li et al., 2024; Wu et al., 2013). However, these data should be interpreted as pathway-level associations rather than evidence that these genes directly mediate sex-biased liver disease risk.

Several liver EDEGs also mapped to PI3K–Akt signaling, including *Prlr*, *Fgf6*, *Itga1*, *F2r*, *Lama3*, *Gng4*, and *Ccnd1*. Among these, *Prlr* and *Ccnd1* showed higher expression in females. The PI3K–Akt pathway is involved in growth factor signaling, metabolism, cell proliferation, autophagy, and cancer-associated processes(Hoxhaj & Manning, 2020; Kwekel et al., 2017; Montalto & De Amicis, 2020; Standing et al., 2022; Yu et al., 2018). Lysosome-associated genes, including *Sort1*, *Arsa*, *Ctsb*, and *Atp6v0d2*, were also identified among liver EDEGs and are involved in intracellular trafficking, lysosomal function, and protein degradation pathways(Musunuru et al., 2010; Srinivasan et al., 2019; Wilson et al., 2016). Together, these results suggest that liver sexual dimorphism may extend beyond classical xenobiotic and steroid metabolism to include signaling, intracellular transport, and lysosomal regulation(Sun et al., 2013).

Overall, the liver findings support the concept that sexually dimorphic hepatic expression involves coordinated metabolic, detoxification, endocrine, signalling, and intracellular trafficking pathways. Because this study is based on secondary analysis of public microarray datasets and network-level annotation, these results should be considered hypothesis-generating. Future studies using RNA-seq, proteomics, and targeted functional experiments will be needed to determine whether these sex-biased liver genes directly contribute to sex-specific physiological or disease phenotypes.

X-linked sex-biased genes and shared regulatory features.

Compared with autosomal EDEGs, recurrent X-linked EDEGs showed broader cross-tissue recurrence. *Xist*, *Kdm6a*, *Eif2s3x*, *Kdm5c*, and *Ddx3x* were repeatedly detected across tissues, and Xist showed consistently higher expression in females, as expected from its role in X-chromosome inactivation(Crowley et al., 2015; Hadziselimovic et al., 2017; Li et al., 2018). These genes are functionally diverse but are broadly involved in dosage compensation, chromatin modification, transcriptional regulation, translation, and RNA metabolism (Balaton et al., 2018; Cargill et al., 2021; Chang et al., 2006; Dunford et al., 2017; Garieri et al., 2018; Migeon, 2020; Schenkel et al., 2018; Skopkova et al., 2017; Snijders Blok et al., 2015; Tricarico et al., 2020). The repeated detection of these X-linked genes across tissues suggests that X-linked sex-biased expression may contribute to shared regulatory features of sexual dimorphism. In contrast, autosomal EDEGs were more tissue-specific and were often associated with metabolic, transport, endocrine, or immune-related pathways. This distinction supports the idea that autosomal and X-linked sex-biased genes contribute to sexual dimorphism through partially different biological programs.

Candidate regulatory loci and translational interpretation

The eQTL and genotype-expression analyses identified several candidate-associated loci linked to high-confidence sex-biased genes, including loci near Herc2 for Akr1d1, Aaas for Rxfp1, and multiple candidate-associated genes for kidney EDEGs, such as Hao1, Plcb4, Masp1, Fbxo15, Timm21, Mosmo, Acsm5, and Acsm1. These candidate loci were identified through GeneNetwork eQTL mapping, interval analysis, and B6/D2 genotype-expression comparisons. Therefore, they should be interpreted as genomic regions associated with variation in gene expression rather than confirmed regulators.

Several candidate-associated genes were detected in endocrine or metabolic tissues, including adrenal gland, pituitary gland, liver, and kidney. This pattern is consistent with the broader enrichment of sex-biased expression in metabolic and endocrine-related pathways observed in this study. However, correlation and eQTL analyses cannot establish direct regulatory mechanisms(Langer M., 1987; Pauls et al., 2020). Functional validation, such as allele-specific expression analysis, perturbation experiments, or independent transcriptomic datasets, will be required to determine whether these candidate loci directly influence sex-biased gene expression.

Cross-species implications

Cross-species comparison with human transcriptomic data showed partial conservation of sex-biased expression patterns. X-linked EDEGs showed more consistent sex-biased trends across species, whereas autosomal EDEGs showed greater tissue- and species-dependent variability. For example, several mouse liver EDEGs had human orthologs expressed in liver, but the direction and magnitude of sex bias were not always conserved. These findings support the relevance of BXD mouse data for generating hypotheses about human sex-biased biology, while also emphasizing that mouse-to-human extrapolation should be interpreted cautiously.

Overall, this study provides a cross-tissue systems-level view of sex-biased expression in BXD mice. The findings highlight tissue specificity, distinguish autosomal and X-linked patterns, and prioritize candidate-associated loci for future validation. However, because the analyses are based on public microarray datasets and exploratory genetic correlations, the results should be interpreted as hypothesis-generating rather than mechanistic proof.

5 Conclusion

In this study, we re-analyzed public GeneNetwork microarray datasets to characterize sex-biased gene expression across seven BXD mouse tissues. The results showed that sexually dimorphic expression is highly tissue dependent, with liver and endocrine-related tissues showing broader sex-biased transcriptional patterns under the thresholds used. Autosomal EDEGs were largely tissue-specific and were enriched for metabolic, transport, endocrine, and immune-related functions, whereas recurrent X-linked EDEGs, including Xist, Kdm6a, Eif2s3x, Kdm5c, and Ddx3x, showed broader cross-tissue recurrence and were associated with core regulatory processes.

The liver contained the largest EDEG set and showed enrichment for xenobiotic metabolism, steroid metabolism, lipid metabolism, signaling, and lysosomal pathways. Candidate-associated loci identified through eQTL and genotype-expression analyses provide potential targets for future studies, but these findings should be considered hypothesis-generating rather than mechanistic proof.

Overall, this study provides a cross-tissue systems-level overview of sex-biased expression in BXD mice and highlights both tissue-specific autosomal programs and recurrent X-linked regulatory features. Future RNA-seq, single-cell, proteomic, epigenomic, and functional validation studies will be needed to confirm these candidate genes and clarify their roles in sex-specific physiology and disease.

Declarations

Funding

This work was partially supported by funding from University of Tennessee Health Science Center (R073290109, R073290110) to WG in Memphis, TN, USA; by the Second Affiliated Hospital of Zhengzhou University(202304121) to JMM; and by funding from National Nature Scientific Foundation of China (81770639, 82070657), Applied Technology Research and Development Project of Heilongjiang Province (GA20C019), Outstanding Youth Funds of the First Affiliated Hospital of Harbin Medical University (HYD2020JQ0006), Research Projects of Chinese Research Hospital Association (Y2019FH-DTCC-SB1) to G. Wang in Harbin, Heilongjiang, China.

Conflict of interest

The authors declared no potential conflicts of interest.

Ethics approval and consent to participate

Ethics approval is not applicable

Consent for publication

All authors have read and approved the final manuscript and consent to its publication.

Data availability

The datasets analysed in this study are publicly available. Transcriptomic data from BXD recombinant inbred mouse strains were obtained from the GeneNetwork database (https://www.genenetwork.org). Human transcriptome data used for validation were obtained from the Genotype-Tissue Expression

(GTEx) project (https://gtexportal.org/home/) and The Cancer Genome Atlas (TCGA) Research Network (https://www.cancer.gov/tcga).

SNP data were obtained from Ensembl (http://useast.ensembl.org/). Candidate gene information was sourced from GeneCards (https://www.genecards.org/) and UniProt (https://www.uniprot.org/). Protein-protein interaction data were analysed using STRING (https://string-db.org/). GO and KEGG enrichment analyses were performed using STRING and the Database for Annotation, Visualization, and Integrated Discovery (DAVID v6.8; https://david.ncifcrf.gov/). Protein sequence data were downloaded from the NCBI Protein database (https://www.ncbi.nlm.nih.gov/protein).

All data generated or analysed during this study are included in this published article and its supplementary tables and figures.

Author Contribution

Conceived and designed the experiments: WG, LW, JJ, GW. Performed the experiments: JM, LW, GY, CF, LY, WD, YJ. Analyzed the data: JM, LW, GY, LY, CT, DZL, YJ, HF, CF. Contributed reagents/materials/analysis tools: LL, AB, MJ, WG, GW. Wrote the paper: JM, LW, GY, WG. Revised the manuscript: AB, MJ, HF, LY, WD, DZL, CT, LL, JJ, YJ, GW, WG. Read and approved the manuscript: All authors

Acknowledgement

The authors thank Dr. Robert Williams for the resources at GeneNetwork and for technical assistance with the data analysis. We thank the following people and their colleagues who contributed the data to GeneNetwork: Lu Lu, Kristin M Hamre, Gerald I Byrne, Melloni Cook, Yue Huang, Yueying Zhang, Wenli Lu, Xiaoyun Liu, and Yonghui Ma (UTHSC); Glenn D. Rosen at Beth Israel Deaconess Medical Center; Eric S. Orwoll and Robert F. Klein (Oregon Health and Sciences University); Patrizia Porcu (University of North Carolina School of Medicine); Richard J Webby (St. Jude Children's Research Hospital); Elissa J Chesler (Oak Ridge National Laboratory/The Jackson laboratory); Gary A. Churchill (The Jackson Laboratory); David Threadgill (Texas A&M University); Arimantas Lionikas (University of Aberdeen); Dan Goldowitz (University of British Columbia); Sara R Jones (Wake Forest University Health Sciences); Richard W. Moyer (University of Florida College of Medicine); Johan Auwerx (School of Life Sciences, École Polytechnique Fédérale de Lausanne); Leslie C. Jones (The Pennsylvania State University); Martina Buresova (Institute of Clinical and Experimental Medicine, Prague); Boris Tabakoff (University of Colorado); Alan D Attie (University of Wisconsin); and Amanda J. Myers (University of Miami).

Data Availability

The datasets analysed in this study are publicly available. Mouse transcriptomic data were obtained from GeneNetwork (https://www.genenetwork.org). Human transcriptomic data were obtained from GTEx (https://gtexportal.org/home/). SNP and gene annotation data were obtained from Ensembl, GeneCards, UniProt, STRING, DAVID, and NCBI Protein. All data sources are described in the manuscript.

References

1. Appikonda S, Thakkar KN, Barton MC (2016) Regulation of gene expression in human cancers by TRIM24. Drug Discov Today Technol 19:57–63. https://doi.org/10.1016/j.ddtec.2016.05.001
2. Ashburner M, Ball CA, Blake JA, Botstein D, Butler H, Cherry JM, Davis AP, Dolinski K, Dwight SS, Eppig JT, Harris MA, Hill DP, Issel-Tarver L, Kasarskis A, Lewis S, Matese JC, Richardson JE, Ringwald M, Rubin GM, Sherlock G (2000) Gene Ontology: tool for the unification of biology. Nat Genet 25(1):25–29. https://doi.org/10.1038/75556
3. Balaton BP, Dixon-McDougall T, Peeters SB, Brown CJ (2018) The eXceptional nature of the X chromosome. Hum Mol Genet 27(R2):R242–R249. https://doi.org/10.1093/hmg/ddy148
4. Barnard L, Nikolaou N, Louw C, Schiffer L, Gibson H, Gilligan LC, Gangitano E, Snoep J, Arlt W, Tomlinson JW, Storbeck KH (2020) The A-ring reduction of 11-ketotestosterone is efficiently catalysed by AKR1D1 and SRD5A2 but not SRD5A1. J Steroid Biochem Mol Biol 202:105724. https://doi.org/10.1016/j.jsbmb.2020.105724
5. Benoist M, Gaillard S, Castets F (2006) The striatin family: a new signaling platform in dendritic spines. J Physiol Paris 99(2–3):146–153. https://doi.org/10.1016/j.jphysparis.2005.12.006
6. Cao Y, Wang L, Wang CY, Ye J, Wang Y, Li T, Garcia-Godoy F, Sun D, Gu W, Postlethwaite AE (2018) Sex Differences in Correlation with Gene Expression Levels between Ifi200 Family Genes and Four Sets of Immune Disease-Relevant Genes. *J Immunol Res*, *2018*, 1290814. https://doi.org/10.1155/2018/1290814
7. Care A, Bellenghi M, Matarrese P, Gabriele L, Salvioli S, Malorni W (2018) Sex disparity in cancer: roles of microRNAs and related functional players. Cell Death Differ 25(3):477–485. https://doi.org/10.1038/s41418-017-0051-x
8. Cargill M, Morales A, Ravishankar S, Warren E (2021) RNA helicase, DDX3X, is actively recruited to sites of DNA damage in live cells. DNA Repair 103:103137. https://doi.org/10.1016/j.dnarep.2021.103137
9. Chang PC, Chi CW, Chau GY, Li FY, Tsai YH, Wu JC, Lee W, Y. H (2006) DDX3, a DEAD box RNA helicase, is deregulated in hepatitis virus-associated hepatocellular carcinoma and is involved in cell growth control. Oncogene 25(14):1991–2003. https://doi.org/10.1038/sj.onc.1209239
10. Chen L, Chou CL, Yang CR, Knepper MA (2023) Multiomics Analyses Reveal Sex Differences in Mouse Renal Proximal Subsegments. J Am Soc Nephrol 34(5):829–845. https://doi.org/10.1681/asn.0000000000000089

11. Chen S, Liu R, Mo CK, Wendl MC, Houston A, Lal P, Zhao Y, Caravan W, Shinkle AT, Abedin-Do A, Naser Al Deen N, Sato K, Li X, Targino da Costa ALN, Li Y, Karpova A, Herndon JM, Artyomov MN, Rubin JB, Chen F (2025) Multi-omic and spatial analysis of mouse kidneys highlights sex-specific differences in gene regulation across the lifespan. Nat Genet 57(5):1213–1227. https://doi.org/10.1038/s41588-025-02161-x
12. Colvin PL Jr, Adams WJ, Sorci-Thomas MR MG (1998) Sex steroids increase cholesterol 7alpha-hydroxylase mRNA in nonhuman primates. Metabolism 47 4391–395. https://doi.org/10.1016/s0026-0495(98)90048-8
13. Conforto TL, Waxman DJ (2012) Sex-specific mouse liver gene expression: genome-wide analysis of developmental changes from pre-pubertal period to young adulthood. Biol Sex Differ 3:9. https://doi.org/10.1186/2042-6410-3-9
14. Consortium GT, Laboratory DA, Center C, Working -Analysis, Working GSMgroups-Analysis, Enhancing G, Fund Gg, Nci NIHCN, Nhgri N, Nimh N, Nida N, Site BCS, Biospecimen Core N, Resource V, Brain Bank Repository-University of Miami Brain, Endowment B, Biomedical-Project L, Study M, Visualization E, Montgomery EBI (2017) S. B. Genetic effects on gene expression across human tissues. *Nature*, *550*(7675), 204–213. https://doi.org/10.1038/nature24277
15. Consortium TGO, Aleksander SA, Balhoff J, Carbon S, Cherry JM, Drabkin HJ, Ebert D, Feuermann M, Gaudet P, Harris NL, Hill DP, Lee R, Mi H, Moxon S, Mungall CJ, Muruganugan A, Mushayahama T, Sternberg PW, Thomas PD, Westerfield M (2023) The Gene Ontology knowledgebase in 2023. Genetics 224(1). https://doi.org/10.1093/genetics/iyad031
16. Consortium TU (2024) UniProt: the Universal Protein Knowledgebase in 2025. Nucleic Acids Res 53(D1):D609–D617. https://doi.org/10.1093/nar/gkae1010
17. Crowley JJ, Zhabotynsky V, Sun W, Huang S, Pakatci IK, Kim Y, Wang JR, Morgan AP, Calaway JD, Aylor DL, Yun Z, Bell TA, Buus RJ, Calaway ME, Didion JP, Gooch TJ, Hansen SD, Robinson NN, Shaw GD, de Pardo-Manuel F (2015) Analyses of allele-specific gene expression in highly divergent mouse crosses identifies pervasive allelic imbalance. Nat Genet 47(4):353–360. https://doi.org/10.1038/ng.3222
18. Cunningham F, Allen JE, Allen J, Alvarez-Jarreta J, Amode MR, Armean IM, Austine-Orimoloye O, Azov AG, Barnes I, Bennett R, Berry A, Bhai J, Bignell A, Billis K, Boddu S, Brooks L, Charkhchi M, Cummins C, Fioretto DR, Flicek L, P (2022) Ensembl 2022. Nucleic Acids Res 50(D1):D988–d995. https://doi.org/10.1093/nar/gkab1049
19. Dale KEaB (2020) Endocrine Control of Reproduction: Controlled Ovarian Hyperstimulation for ART. In K. Elder & B. Dale (Eds.), *In-Vitro Fertilization* (4 ed., pp. 40–52). Cambridge University Press. https://doi.org/DOI: 10.1017/9781108611633.003
20. Database resources of the National Center for Biotechnology Information (2016) Nucleic Acids Res 44(D1):D7–19. https://doi.org/10.1093/nar/gkv1290
21. Dunford A, Weinstock DM, Savova V, Schumacher SE, Cleary JP, Yoda A, Sullivan TJ, Hess JM, Gimelbrant AA, Beroukhim R, Lawrence MS, Getz G, Lane AA (2017) Tumor-suppressor genes that escape from X-inactivation contribute to cancer sex bias. Nat Genet 49(1):10–16. https://doi.org/10.1038/ng.3726
22. Gal-Oz ST, Maier B, Yoshida H, Seddu K, Elbaz N, Czysz C, Zuk O, Stranger BE, Ner-Gaon H, Shay T (2019) ImmGen report: sexual dimorphism in the immune system transcriptome. Nat Commun 10(1):4295. https://doi.org/10.1038/s41467-019-12348-6
23. Garieri M, Stamoulis G, Blanc X, Falconnet E, Ribaux P, Borel C, Santoni F, Antonarakis SE (2018) Extensive cellular heterogeneity of X inactivation revealed by single-cell allele-specific expression in human fibroblasts. Proc Natl Acad Sci U S A 115(51):13015–13020. https://doi.org/10.1073/pnas.1806811115
24. Garza AE, Pojoga LH, Moize B, Hafiz WM, Opsasnick LA, Siddiqui WT, Horenstein M, Adler GK, Williams GH, Khalil RA (2015) Critical Role of Striatin in Blood Pressure and Vascular Responses to Dietary Sodium Intake. Hypertension 66(3):674–680. https://doi.org/10.1161/HYPERTENSIONAHA.115.05600
25. Gatti D, Maki A, Chesler EJ, Kirova R, Kosyk O, Lu L, Manly KF, Williams RW, Perkins A, Langston MA, Threadgill DW, Rusyn I (2007) Genome-level analysis of genetic regulation of liver gene expression networks. Hepatology (Baltimore MD) 46(2):548–557. https://doi.org/10.1002/hep.21682
26. Gatti DM, Zhao N, Chesler EJ, Bradford BU, Shabalin AA, Yordanova R, Lu L, Rusyn I (2010) Sex-specific gene expression in the BXD mouse liver. Physiol Genomics 42(3):456–468. https://doi.org/10.1152/physiolgenomics.00110.2009
27. Gay NR, Gloudemans M, Antonio ML, Abell NS, Balliu B, Park Y, Martin AR, Musharoff S, Rao AS, Aguet F, Barbeira AN, Bonazzola R, Hormozdiari F, Consortium GT, Ardlie KG, Brown CD, Im HK, Lappalainen T, Wen X, Montgomery SB (2020) Impact of admixture and ancestry on eQTL analysis and GWAS colocalization in GTEx. Genome Biol 21(1):233. https://doi.org/10.1186/s13059-020-02113-0
28. Giretti MS, Simoncini T (2008) Rapid regulatory actions of sex steroids on cell movement through the actin cytoskeleton. Steroids 73(9–10):895–900. https://doi.org/10.1016/j.steroids.2008.01.011
29. Gupta T, Connors M, Tan JW, Manosroi W, Ahmed N, Ting PY, Garza AE, Romero JR, Hopkins PN, Williams JS, Williams GH (2017) Striatin Gene Polymorphic Variants Are Associated With Salt Sensitive Blood Pressure in Normotensives and Hypertensives. Am J Hypertens 31(1):124–131. https://doi.org/10.1093/ajh/hpx146
30. Hadziselimovic F, Gegenschatz-Schmid K, Verkauskas G, Demougin P, Bilius V, Dasevicius D, Stadler MB (2017) GnRHa Treatment of Cryptorchid Boys Affects Genes Involved in Hormonal Control of the HPG Axis and Fertility. Sex Dev 11(3):126–136. https://doi.org/10.1159/000471937
31. Handelsman DJ, Hirschberg AL, Bermon S (2018) Circulating Testosterone as the Hormonal Basis of Sex Differences in Athletic Performance. Endocr Rev 39(5):803–829. https://doi.org/10.1210/er.2018-00020
32. Hoxhaj G, Manning BD (2020) The PI3K-AKT network at the interface of oncogenic signalling and cancer metabolism. Nat Rev Cancer 20(2):74–88. https://doi.org/10.1038/s41568-019-0216-7
33. Ingleby FC, Flis I, Morrow EH (2014) Sex-biased gene expression and sexual conflict throughout development. Cold Spring Harb Perspect Biol 7(1):a017632. https://doi.org/10.1101/cshperspect.a017632

34. Islami F, Ward EM, Sung H, Cronin KA, Tangka FKL, Sherman RL, Zhao J, Anderson RN, Henley SJ, Yabroff KR, Jemal A, Benard VB (2021) Annual Report to the Nation on the Status of Cancer, Part 1: National Cancer Statistics. *JNCI: Journal of the National Cancer Institute*, *113*(12), 1648–1669. https://doi.org/10.1093/jnci/djab131
35. Iwai N, Mannami KT, Higaki T, Ogihara J, Kokame T, Ogata K, Baba J S (2002) Association between SAH, an acyl-CoA synthetase gene, and hypertriglyceridemia, obesity, and hypertension. Circulation 105(1). https://doi.org/10.1161/hc0102.101780
36. Kanehisa M, Furumichi M, Sato Y, Matsuura Y, Ishiguro-Watanabe M (2025) KEGG: biological systems database as a model of the real world. Nucleic Acids Res 53(D1):D672–d677. https://doi.org/10.1093/nar/gkae909
37. Khodursky S, Jiang CS, Zheng EB, Vaughan R, Schrider DR, Zhao L (2022) Sex differences in interindividual gene expression variability across human tissues. PNAS Nexus 1(5):pgac243. https://doi.org/10.1093/pnasnexus/pgac243
38. Klein SL, Flanagan KL (2016) Sex differences in immune responses. Nat Rev Immunol 16(10):626–638. https://doi.org/10.1038/nri.2016.90
39. Krumsiek J, Mittelstrass K, Do KT, Stückler F, Ried J, Adamski J, Peters A, Illig T, Kronenberg F, Friedrich N, Nauck M, Pietzner M, Mook-Kanamori DO, Suhre K, Gieger C, Grallert H, Theis FJ, Kastenmüller G (2015) Gender-specific pathway differences in the human serum metabolome. Metabolomics 11(6):1815–1833. https://doi.org/10.1007/s11306-015-0829-0
40. Kwekel JC, Vijay V, Han T, Moland CL, Desai VG, Fuscoe JC (2017) Sex and age differences in the expression of liver microRNAs during the life span of F344 rats. Biol Sex Differ 8:6. https://doi.org/10.1186/s13293-017-0127-9
41. Langer M, I. CL, Csomós OL, Crepaldi G G. (eds) (1987) Assessment and Management of Hepatobiliary Disease. Springer, Berlin, Heidelberg. https://doi.org/10.1007/978-3-642-72631-6_29
42. Lau-Corona D, Bae WK, Hennighausen L, Waxman DJ (2020) Sex-biased genetic programs in liver metabolism and liver fibrosis are controlled by EZH1 and EZH2. PLoS Genet 16(5):e1008796. https://doi.org/10.1371/journal.pgen.1008796
43. Li AX, Martin TA, Lane J, Jiang WG (2024) Cellular Impacts of Striatins and the STRIPAK Complex and Their Roles in the Development and Metastasis in Clinical Cancers (Review). *Cancers*, *16*(1), 76. https://www.mdpi.com/2072-6694/16/1/76
44. Li C, Wan L, Liu Z, Xu G, Wang S, Su Z, Zhang Y, Zhang C, Liu X, Lei Z, Zhang HT (2018) Long non-coding RNA XIST promotes TGF-β-induced epithelial-mesenchymal transition by regulating miR-367/141-ZEB2 axis in non-small-cell lung cancer. Cancer Lett 418:185–195. https://doi.org/10.1016/j.canlet.2018.01.036
45. Lopes-Ramos CM, Chen CY, Kuijjer ML, Paulson JN, Sonawane AR, Fagny M, Platig J, Glass K, Quackenbush J, DeMeo DL (2020) Sex Differences in Gene Expression and Regulatory Networks across 29 Human Tissues. Cell Rep 31(12):107795. https://doi.org/10.1016/j.celrep.2020.107795
46. Mank JE (2017) The transcriptional architecture of phenotypic dimorphism. Nat Ecol Evol 1(1):0006. https://doi.org/10.1038/s41559-016-0006
47. Matsuo H, Kanai Y, Kim JY, Chairoungdua A, Kim DK, Inatomi J, Shigeta Y, Ishimine H, Chaekuntode S, Tachampa K, Choi HW, Babu E, Fukuda J, Endou H (2002) Identification of a novel Na+-independent acidic amino acid transporter with structural similarity to the member of a heterodimeric amino acid transporter family associated with unknown heavy chains. J Biol Chem 277(23):21017–21026. https://doi.org/10.1074/jbc.M200019200
48. Mele M, Ferreira PG, Reverter F, DeLuca DS, Monlong J, Sammeth M, Young TR, Goldmann JM, Pervouchine DD, Sullivan TJ, Johnson R, Segre AV, Djebali S, Niarchou A, Consortium GT, Wright FA, Lappalainen T, Calvo M, Getz G, Guigo R (2015) Human genomics. The human transcriptome across tissues and individuals. Science 348(6235):660–665. https://doi.org/10.1126/science.aaa0355
49. Migeon BR (2020) X-linked diseases: susceptible females. Genet Sci 22(7):1156–1174. https://doi.org/10.1038/s41436-020-0779-4
50. Montalto FI, De Amicis F (2020) Cyclin D1 in Cancer: A Molecular Connection for Cell Cycle Control, Adhesion and Invasion in Tumor and Stroma. Cells 9(12). https://doi.org/10.3390/cells9122648
51. Mozhui K, Lu L, Armstrong WE, Williams RW (2012) Sex-specific modulation of gene expression networks in murine hypothalamus. Front Neurosci 6:63. https://doi.org/10.3389/fnins.2012.00063
52. Mulligan MK, Mozhui K, Prins P, Williams RW (2017) GeneNetwork: A Toolbox for Systems Genetics. In K. Schughart & R. W. Williams (Eds.), *Systems Genetics: Methods and Protocols* (pp. 75–120). Springer New York. https://doi.org/10.1007/978-1-4939-6427-7_4
53. Musunuru K, Strong A, Frank-Kamenetsky M, Lee NE, Ahfeldt T, Sachs KV, Li X, Li H, Kuperwasser N, Ruda VM, Pirruccello JP, Muchmore B, Prokunina-Olsson L, Hall JL, Schadt EE, Morales CR, Lund-Katz S, Phillips MC, Wong J, Rader DJ (2010) From noncoding variant to phenotype via SORT1 at the 1p13 cholesterol locus. Nature 466(7307):714–719. https://doi.org/10.1038/nature09266
54. Ngo ST, Steyn FJ, McCombe PA (2014) Gender differences in autoimmune disease. Front Neuroendocrinol 35(3):347–369. https://doi.org/10.1016/j.yfrne.2014.04.004
55. Nikolaou N, Gathercole LL, Marchand L, Althari S, Dempster NJ, Green CJ, van de Bunt M, McNeil C, Arvaniti A, Hughes BA, Sgromo B, Gillies RS, Marschall HU, Penning TM, Ryan J, Arlt W, Hodson L, Tomlinson JW (2019) AKR1D1 is a novel regulator of metabolic phenotype in human hepatocytes and is dysregulated in non-alcoholic fatty liver disease. Metabolism 99:67–80. https://doi.org/10.1016/j.metabol.2019.153947
56. Oliva M, Muñoz-Aguirre M, Kim-Hellmuth S, Wucher V, Gewirtz ADH, Cotter DJ, Parsana P, Kasela S, Balliu B, Viñuela A, Castel SE, Mohammadi P, Aguet F, Zou Y, Khramtsova EA, Skol AD, Garrido-Martín D, Reverter F, Brown A, Stranger BE (2020) The impact of sex on gene expression across human tissues. Science 369(6509). https://doi.org/10.1126/science.aba3066
57. Oliveira PA, Chaves CA, Guedes-Pinto R, De-La-Cruz H, Lopes PLF C (2007) Chemical carcinogenesis. Acad Bras Cienc 79:593–616. https://doi.org/10.1590/s0001-37652007000400004
58. Parsch J, Ellegren H (2013) The evolutionary causes and consequences of sex-biased gene expression. Nat Rev Genet 14(2):83–87. https://doi.org/10.1038/nrg3376

59. Pauls SD, Ragheb M, Winter T, Leng S, Taylor CG, Zahradka P, Aukema HM (2020) Spleen Oxylipin and Polyunsaturated Fatty Acid Profiles are Altered by Dietary Source of Polyunsaturated Fatty Acid and by Sex. Lipids 55(3):261–270. https://doi.org/10.1002/lipd.12235
60. Pearson WR (2013) An introduction to sequence similarity (homology) searching. Curr Protoc Bioinf. Chap. 3 https://doi.org/10.1002/0471250953.bi0301s42. Unit3.1
61. Peirce JL, Lu L, Gu J, Silver LM, Williams RW (2004) A new set of BXD recombinant inbred lines from advanced intercross populations in mice. BMC Genet 5:7. https://doi.org/10.1186/1471-2156-5-7
62. Phelps T, Snyder E, Rodriguez E, Child H, Harvey P (2019) The influence of biological sex and sex hormones on bile acid synthesis and cholesterol homeostasis. Biol Sex Differ 10(1):52. https://doi.org/10.1186/s13293-019-0265-3
63. Ransick A, Lindstrom NO, Liu J, Zhu Q, Guo JJ, Alvarado GF, Kim AD, Black HG, Kim J, McMahon AP (2019) Single-Cell Profiling Reveals Sex, Lineage, and Regional Diversity in the Mouse Kidney. Dev Cell 51(3):399–413e397. https://doi.org/10.1016/j.devcel.2019.10.005
64. Regitz-Zagrosek V, Kararigas G (2017) Mechanistic Pathways of Sex Differences in Cardiovascular Disease. Physiol Rev 97(1):1–37. https://doi.org/10.1152/physrev.00021.2015
65. Rich NE, Oji S, Mufti AR, Browning JD, Parikh ND, Odewole M, Mayo H, Singal AG (2018) Racial and Ethnic Disparities in Nonalcoholic Fatty Liver Disease Prevalence, Severity, and Outcomes in the United States: A Systematic Review and Meta-analysis. Clin Gastroenterol Hepatol 16(2):198–210e192. https://doi.org/10.1016/j.cgh.2017.09.041
66. Ruhs S, Nolze A, Hübschmann R, Grossmann C (2017) 30 YEARS OF THE MINERALOCORTICOID RECEPTOR: Nongenomic effects via the mineralocorticoid receptor. J Endocrinol 234(1):T107–T124. https://doi.org/10.1530/joe-16-0659
67. Sabino KR, Petroianu A (2021) Splenectomy is associated with sexual dysfunctions and decreased libido. Sci Rep 11(1):21770. https://doi.org/10.1038/s41598-021-01371-7
68. Safran M, Dalah I, Alexander J, Rosen N, Stein I, Shmoish T, Nativ M, Bahir N, Doniger I, Krug T, Sirota-Madi H, Olender A, Golan T, Stelzer Y, Harel G, A., Lancet D (2010) GeneCards Version 3: the human gene integrator. Database 2010. https://doi.org/10.1093/database/baq020
69. Schenkel LC, Aref-Eshghi E, Skinner C, Ainsworth P, Lin H, Paré G, Rodenhiser DI, Schwartz C, Sadikovic B (2018) Peripheral blood epi-signature of Claes-Jensen syndrome enables sensitive and specific identification of patients and healthy carriers with pathogenic mutations in KDM5C. Clin Epigenetics 10(1):21. https://doi.org/10.1186/s13148-018-0453-8
70. Sherman BT, Hao M, Qiu J, Jiao X, Baseler MW, Lane HC, Imamichi T, Chang W (2022) DAVID: a web server for functional enrichment analysis and functional annotation of gene lists (2021 update). Nucleic Acids Res 50(W1):W216–w221. https://doi.org/10.1093/nar/gkac194
71. Si H, Banga RS, Kapitsinou P, Ramaiah M, Lawrence J, Kambhampati G, Gruenwald A, Bottinger E, Glicklich D, Tellis V, Greenstein S, Thomas DB, Pullman J, Fazzari M, Susztak K (2009) Human and murine kidneys show gender- and species-specific gene expression differences in response to injury. PLoS ONE 4(3):e4802. https://doi.org/10.1371/journal.pone.0004802
72. Skopkova M, Hennig F, Shin BS, Turner CE, Stanikova D, Brennerova K, Stanik J, Fischer U, Henden L, Müller U, Steinberger D, Leshinsky-Silver E, Bottani A, Kurdiova T, Ukropec J, Nyitrayova O, Kolnikova M, Klimes I, Borck G, Kalscheuer VM (2017) EIF2S3 Mutations Associated with Severe X-Linked Intellectual Disability Syndrome MEHMO. Hum Mutat 38(4):409–425. https://doi.org/10.1002/humu.23170
73. Snijders Blok L, Madsen E, Juusola J, Gilissen C, Baralle D, Reijnders MR, Venselaar H, Helsmoortel C, Cho MT, Hoischen A, Vissers LE, Koemans TS, Wissink-Lindhout W, Eichler EE, Romano C, Van Esch H, Stumpel C, Vreeburg M, Smeets E, Kleefstra T (2015) Mutations in DDX3X Are a Common Cause of Unexplained Intellectual Disability with Gender-Specific Effects on Wnt Signaling. Am J Hum Genet 97(2):343–352. https://doi.org/10.1016/j.ajhg.2015.07.004
74. Srinivasan K, Friedman BA, Etxeberria A, Huntley MA, van der Brug MP, Foreman O, Paw JS, Modrusan Z, Beach TG, Serrano GE, Hansen DV (2019) Alzheimer's patient brain myeloid cells exhibit enhanced aging and unique transcriptional activation. J Immunol. https://doi.org/10.1101/610345
75. Standing D, Dandawate P, Anant S (2022) Prolactin receptor signaling: A novel target for cancer treatment - Exploring anti-PRLR signaling strategies. Front Endocrinol (Lausanne) 13:1112987. https://doi.org/10.3389/fendo.2022.1112987
76. Stiles AR, McDonald JG, Bauman DR, Russell DW (2009) CYP7B1: one cytochrome P450, two human genetic diseases, and multiple physiological functions. J Biol Chem 284(42):28485–28489. https://doi.org/10.1074/jbc.R109.042168
77. Sun LY, Spong A, Swindell WR, Fang Y, Hill C, Huber JA, Boehm JD, Westbrook R, Salvatori R, Bartke A (2013) Growth hormone-releasing hormone disruption extends lifespan and regulates response to caloric restriction in mice. Elife 2:e01098. https://doi.org/10.7554/eLife.01098
78. Szklarczyk D, Kirsch R, Koutrouli M, Nastou K, Mehryary F, Hachilif R, Gable AL, Fang T, Doncheva NT, Pyysalo S, Bork P, Jensen LJ, von Mering C (2023) The STRING database in 2023: protein-protein association networks and functional enrichment analyses for any sequenced genome of interest. Nucleic Acids Res 51(D1):D638–d646. https://doi.org/10.1093/nar/gkac1000
79. Tamura KMY (1926) The Effect of Gonadectomy on the Weight of the Kidney, Thymus, and Spleen of Mice. J Exp Biol 3(3):207–223. https://doi.org/https://doi.org/10.1242/jeb.3.3.207
80. Thakkar N, Slizgi JR, Brouwer KLR (2017) Effect of Liver Disease on Hepatic Transporter Expression and Function. J Pharm Sci 106(9):2282–2294. https://doi.org/10.1016/j.xphs.2017.04.053
81. Tricarico R, Nicolas E, Hall MJ, Golemis EA (2020) X- and Y-Linked Chromatin-Modifying Genes as Regulators of Sex-Specific Cancer Incidence and Prognosis. Clin Cancer Res 26(21):5567–5578. https://doi.org/10.1158/1078-0432.CCR-20-1741
82. Valentino RJ, Van Bockstaele E, Bangasser D (2013) Sex-specific cell signaling: the corticotropin-releasing factor receptor model. Trends Pharmacol Sci 34(8):437–444. https://doi.org/10.1016/j.tips.2013.06.004

83. van der Linden C, Jakob S, Gupta P, Dulac C, Santoro SW (2018) Sex separation induces differences in the olfactory sensory receptor repertoires of male and female mice. Nat Commun 9(1):5081. https://doi.org/10.1038/s41467-018-07120-1
84. Vera R, Juan-Vidal O, Safont-Aguilera MJ, de la Peña FA, Del Alba AG (2023) Sex differences in the diagnosis, treatment and prognosis of cancer: the rationale for an individualised approach. Clin Transl Oncol 25(7):2069–2076. https://doi.org/10.1007/s12094-023-03112-w
85. Vessey DA, Warren KM RS (1999) Characterization of the CoA ligases of human liver mitochondria catalyzing the activation of short- and medium-chain fatty acids and xenobiotic carboxylic acids. Biochim Biophys Acta 1428(1422–1423):1455–1462. https://doi.org/10.1016/s0304-4165(99)00088-4
86. Voskuhl RR, Sawalha AH, Itoh Y (2018) Sex chromosome contributions to sex differences in multiple sclerosis susceptibility and progression. Mult Scler 24(1):22–31. https://doi.org/10.1177/1352458517737394
87. Wang L, Lu W, Zhang L, Huang Y, Scheib R, Liu X, Myers L, Lu L, Farber CR, Liu G, Wang CY, Deng H, Williams RW, Wang Y, Gu W, Jiao Y (2014) Trps1 differentially modulates the bone mineral density between male and female mice and its polymorphism associates with BMD differently between women and men. PLoS ONE 9(1):e84485. https://doi.org/10.1371/journal.pone.0084485
88. Waxman DJ, O'Connor C (2006) Growth hormone regulation of sex-dependent liver gene expression. Mol Endocrinol 20(11):2613–2629. https://doi.org/10.1210/me.2006-0007
89. Werner RJ, Schultz BM, Huhn JM, Jelinek J, Madzo J, Engel N (2017) Sex chromosomes drive gene expression and regulatory dimorphisms in mouse embryonic stem cells. Biol Sex Differ 8(1):28. https://doi.org/10.1186/s13293-017-0150-x
90. Wilson CM, Naves T, Akhrass A, Vincent H, Melloni F, Bonnaud B, Lalloue F, F., Jauberteau MO (2016) A new role under sortilin's belt in cancer. Commun Integr Biol 9(1):e1130192. https://doi.org/10.1080/19420889.2015.1130192
91. Wu YM, Su F, Kalyana-Sundaram S, Khazanov N, Ateeq B, Cao X, Lonigro RJ, Vats P, Wang R, Lin SF, Cheng AJ, Kunju LP, Siddiqui J, Tomlins SA, Wyngaard P, Sadis S, Roychowdhury S, Hussain MH, Feng FY, Chinnaiyan AM (2013) Identification of targetable FGFR gene fusions in diverse cancers. Cancer Discov 3(6):636–647. https://doi.org/10.1158/2159-8290.CD-13-0050
92. Yahyaoui R, Perez-Frias J (2019) Amino Acid Transport Defects in Human Inherited Metabolic Disorders. Int J Mol Sci 21(1). https://doi.org/10.3390/ijms21010119
93. Yu C, Li WB, Liu JB, Lu JW, Feng JF (2018) Autophagy: novel applications of nonsteroidal anti-inflammatory drugs for primary cancer. Cancer Med 7(2):471–484. https://doi.org/10.1002/cam4.1287

Figures

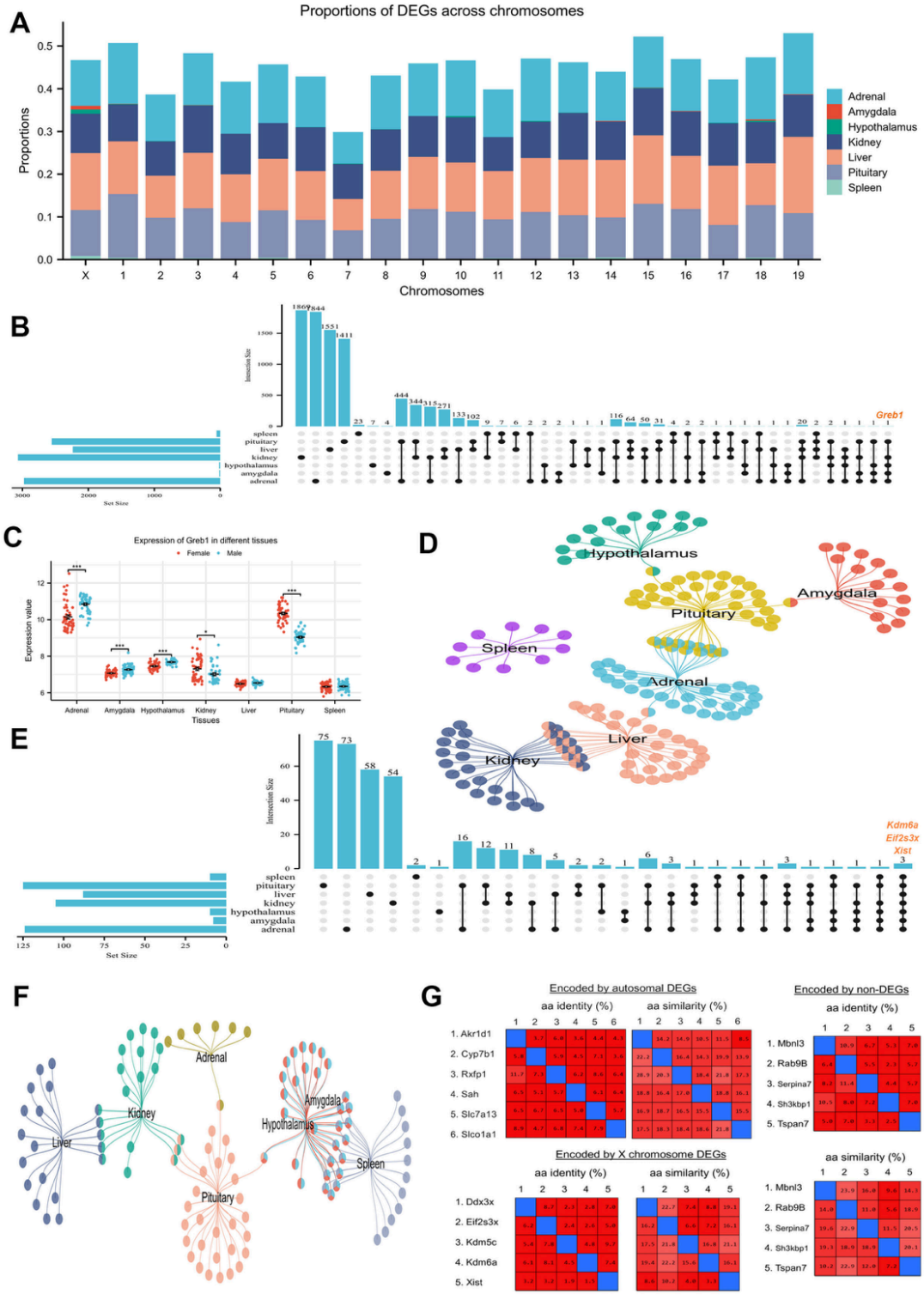


Figure 1

Global landscape of sex-biased gene expression across seven BXD mouse tissues. (**A**) Proportion of sex-biased differentially expressed probes by chromosome across seven tissues. The x-axis shows chromosomes X and 1–19, and the y-axis shows the percentage of probes with Bonferroni-adjusted q < 0.05. (**B**) UpSet plot showing shared and tissue-specific autosomal DEGs across tissues. Bar plots indicate DEG set sizes and intersection sizes. (**C**) Expression patterns of *Greb1*, the most recurrent autosomal DEG, detected in adrenal gland, amygdala, hypothalamus, kidney, and pituitary gland datasets. (**D**) Functional enrichment network of autosomal DEGs based on shared GO and KEGG terms across tissues. Nodes represent enriched terms, and edges indicate shared enrichment terms between tissues. (**E**) UpSet plot showing shared and tissue-specific X-linked DEGs across tissues. Recurrent X-linked genes included *Xist*, *Kdm6a*, *Eif2s3x*, *Kdm5c*, and *Ddx3x*. (**F**) Functional enrichment network of X-linked DEGs based on shared GO and KEGG terms across tissues. (**G)**Pairwise amino acid identity and similarity among proteins encoded by selected recurrent sex-biased genes. Heatmaps show sequence identity and similarity scores between protein pairs; color intensity indicates the degree of similarity.

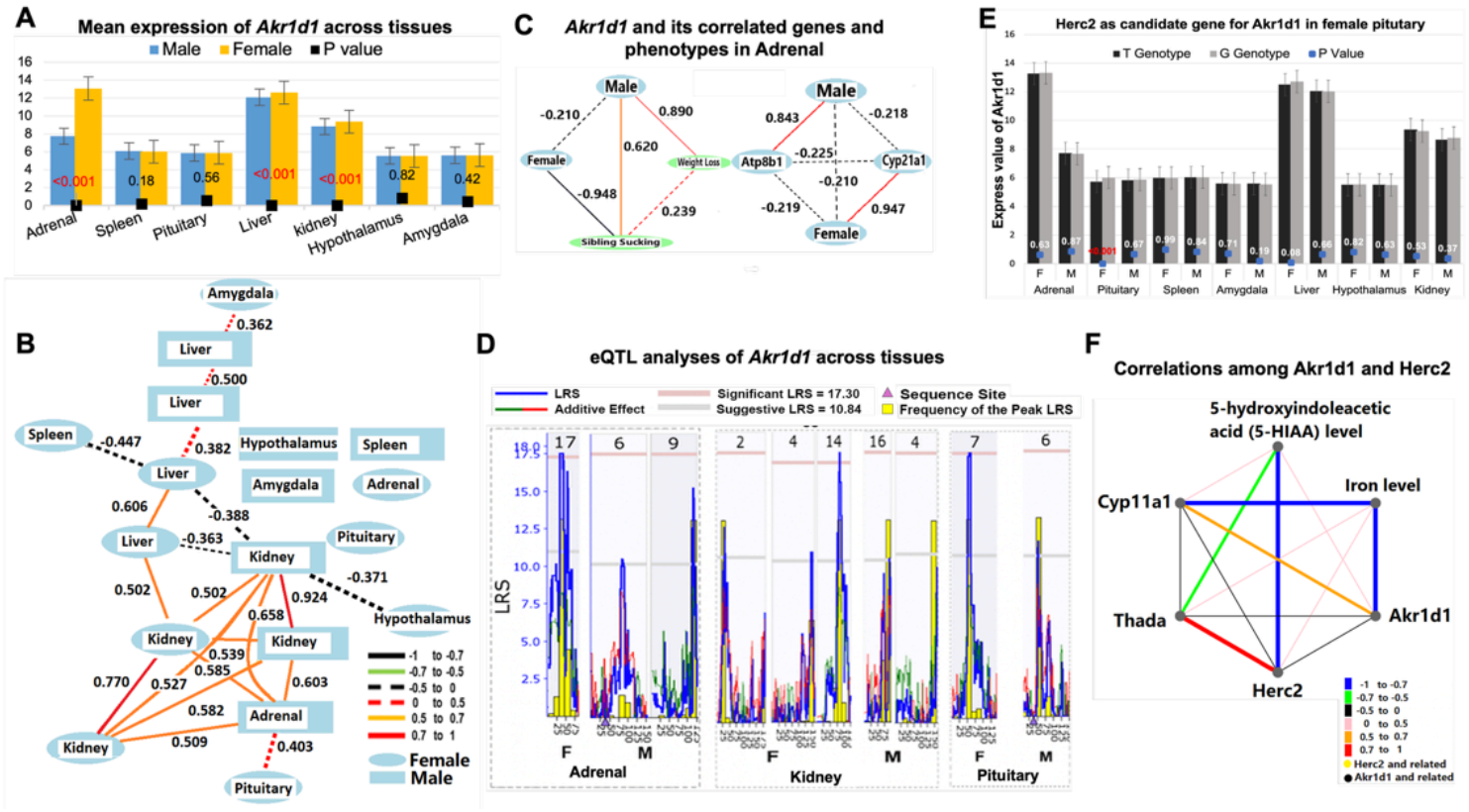


Figure 2

Sex-biased expression and candidate-associated loci of Akr1d1. (**A**) Mean *Akr1d1* expression across seven tissues in male and female mice. Significant sex differences were detected in adrenal gland, kidney, and liver datasets, with the strongest difference observed in adrenal gland. (**B**) Cross-tissue correlation analysis of *Akr1d1* expression across the seven analyzed tissues. Correlation coefficients were calculated separately by sex. (**C**) Gene–phenotype correlation network for adrenal gland *Akr1d1*. Nodes represent *Akr1d1*, top-associated genes, and top-associated phenotypes. Edge labels indicate Pearson correlation coefficients. (**D**) eQTL summary for *Akr1d1*. Only loci exceeding GeneNetwork suggestive or significant LRS thresholds are shown. (**E**) Genotype-expression comparison of *Akr1d1*expression at the *Herc2*-associated locus. B6- and D2-associated alleles were compared using t-test-based genotype-expression analysis. (**F**) Correlation network involving *Akr1d1*, *Herc2*, and their top-associated genes and phenotypes. These analyses were exploratory and do not establish direct regulation.

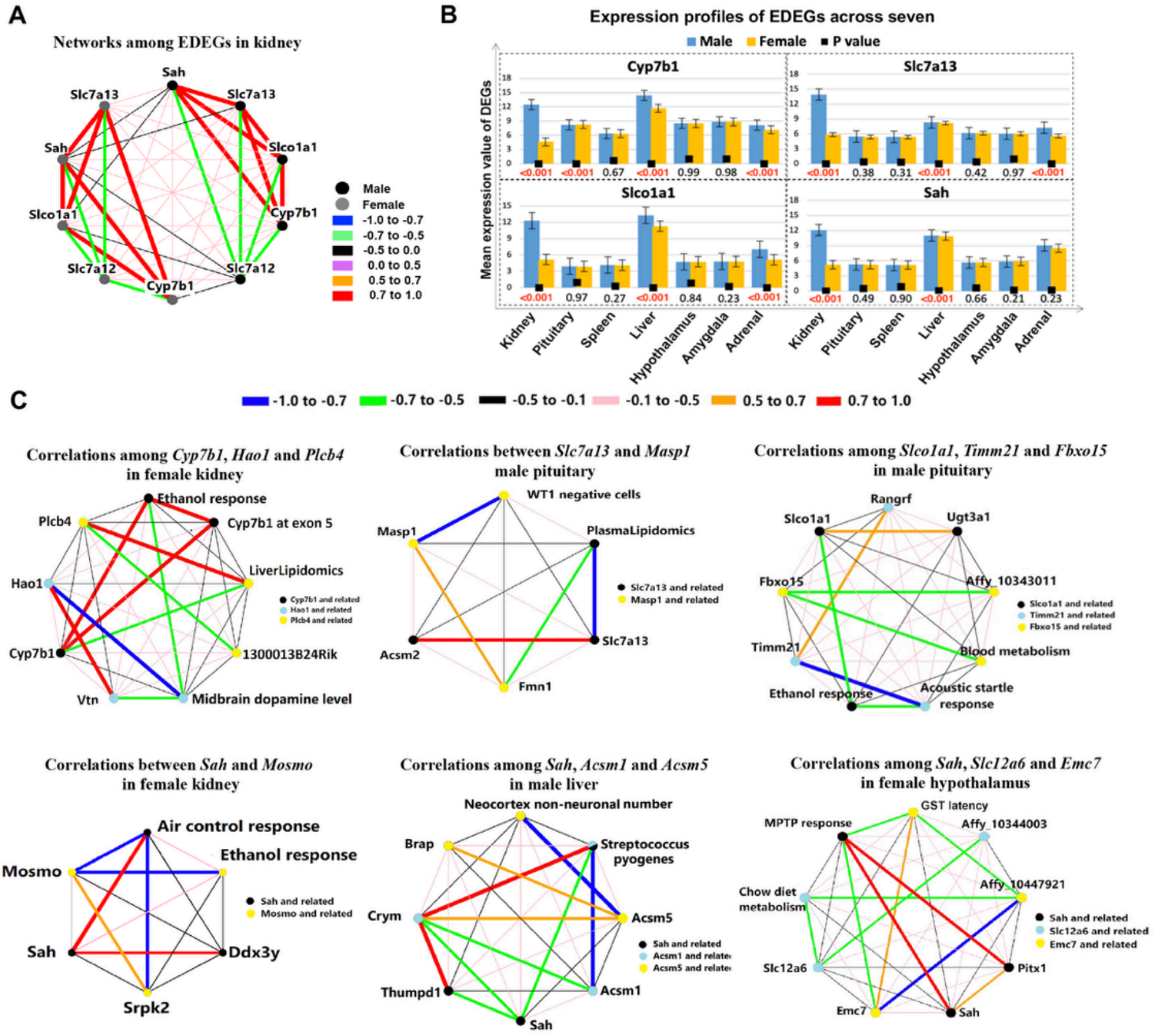


Figure 3

Kidney-associated EDEGs and candidate-associated networks. (**A**) Correlation network among kidney EDEGs. Nodes represent kidney-associated EDEGs, and edges represent Pearson correlations between gene expression traits. Edge thickness indicates correlation strength. (**B**) Mean expression of kidney-associated EDEGs across seven tissues. Genes shown include *Cyp7b1*, *Slc7a13*, *Slco1a1*, and *Acsm3*. Sex-biased expression was assessed independently within each tissue. (**C**) Network analysis integrating kidney EDEGs with candidate-associated genes and top-associated phenotypes. Nodes represent EDEGs, candidate-associated genes, and GeneNetwork phenotypes. Edges represent Pearson correlations. These networks summarize exploratory associations and should not be interpreted as direct regulatory interactions.

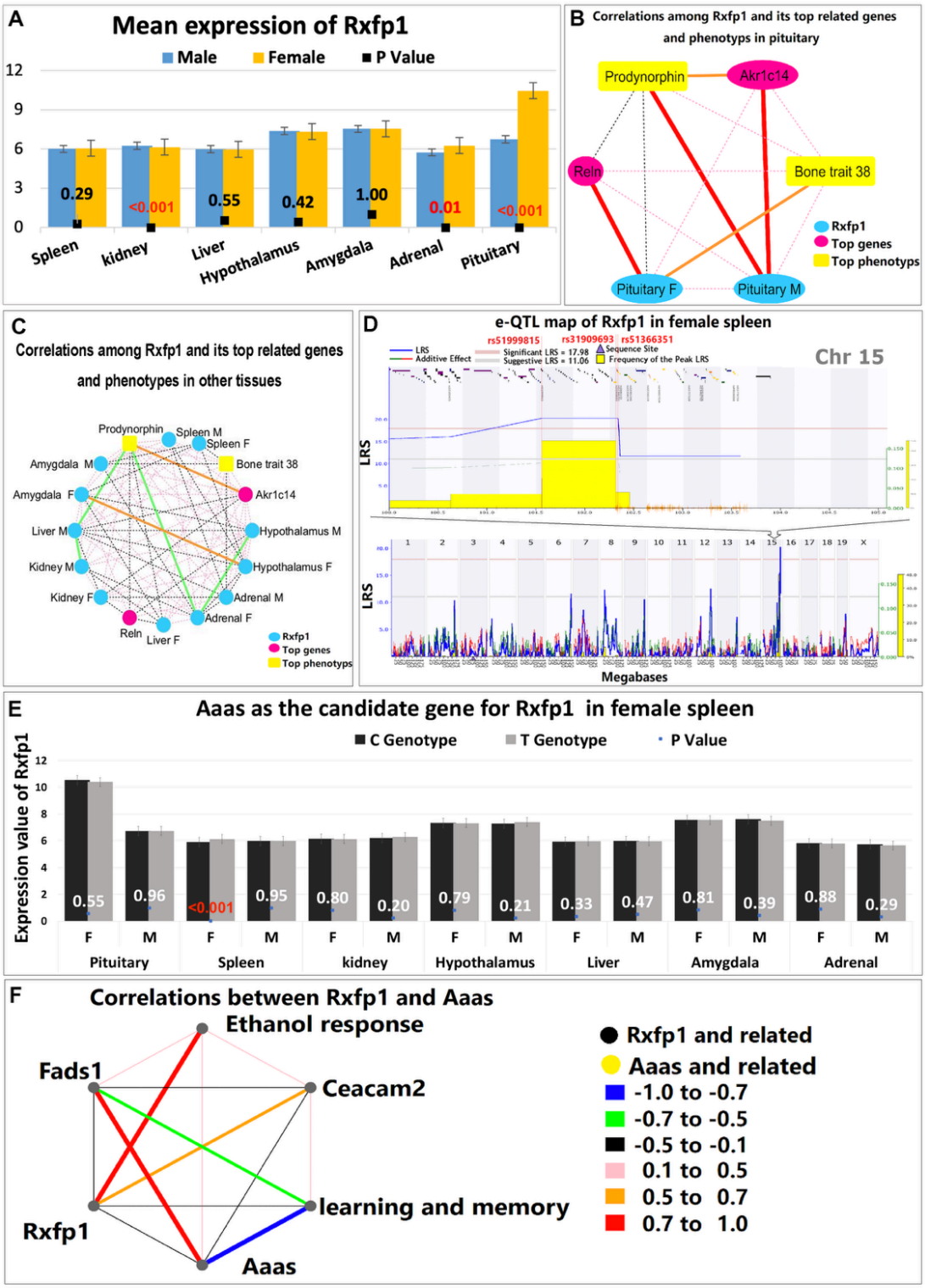


Figure 4

Sex-biased expression and candidate-associated locus of Rxfp1. (**A**) Mean *Rxfp1*expression across seven tissues in male and female mice. Significant sex-biased expression was observed in pituitary gland, kidney, and adrenal gland datasets. (**B**) Gene–phenotype correlation network for pituitary *Rxfp1*. Nodes represent *Rxfp1*, top-associated genes, and top-associated phenotypes. (**C**) Cross-tissue correlation networks showing tissue- and sex-dependent associations of *Rxfp1*expression with selected genes and phenotypes. (**D**) eQTL analysis of *Rxfp1* in the female spleen dataset. A suggestive eQTL was identified on chromosome 15. (**E**) Genotype-expression comparison of *Rxfp1* expression at the *Aaas*-associated locus in the female spleen dataset. (**F**) Correlation network involving *Rxfp1*, *Aaas*, and their top-associated genes and phenotypes. No strong direct correlation between *Rxfp1* and *Aaas*expression was observed.

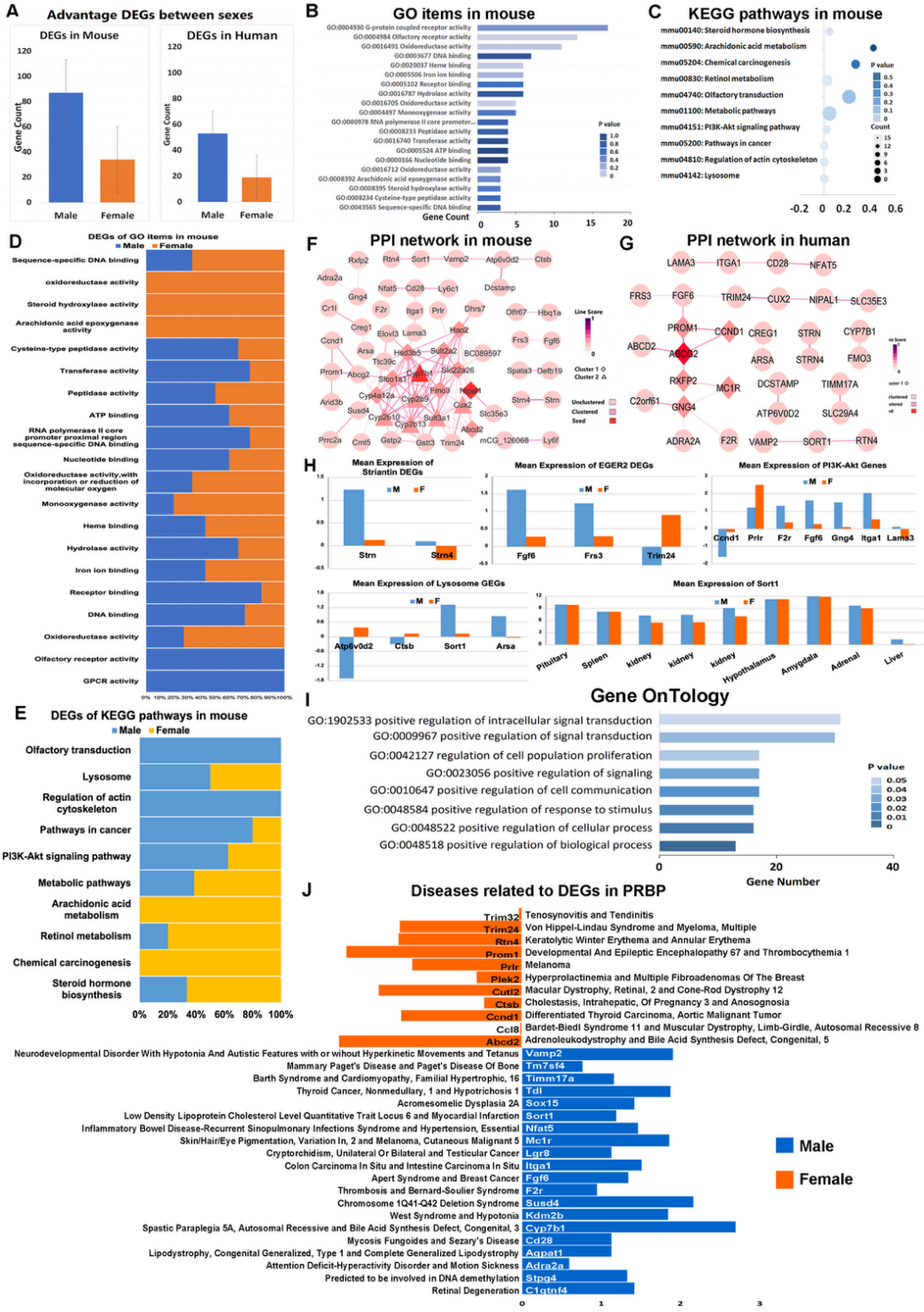


Figure 5

Liver EDEGs, functional enrichment, and human-relevant annotation. (**A**) Numbers of male- and female-biased liver EDEGs in mouse datasets and corresponding human-relevant genes. (**B**) Top enriched GO terms among liver EDEGs. The x-axis shows gene counts, and color intensity represents enrichment significance. (**C**) KEGG pathway enrichment of liver EDEGs. Circle size represents gene count, and color intensity represents enrichment significance. (**D**) Sex-bias distribution of liver EDEGs across enriched GO terms. (**E**) Sex-bias distribution of liver EDEGs across enriched KEGG pathways. (**F**) Protein–protein interaction network of mouse liver EDEGs. Nodes represent proteins encoded by liver EDEGs, and edges represent STRING protein–protein associations. Clustered modules are highlighted. (**G**) Protein–protein interaction network of human-relevant liver EDEGs. Nodes represent human orthologs or corresponding human-expressed genes. (**H**) Expression patterns of liver EDEGs within selected functional modules and pathways. (**I**) Enriched GO terms among human-relevant liver EDEGs. (**J**) Sex-biased genes associated with positive regulation of biological processes. Bars indicate relative mean expression differences between sexes.

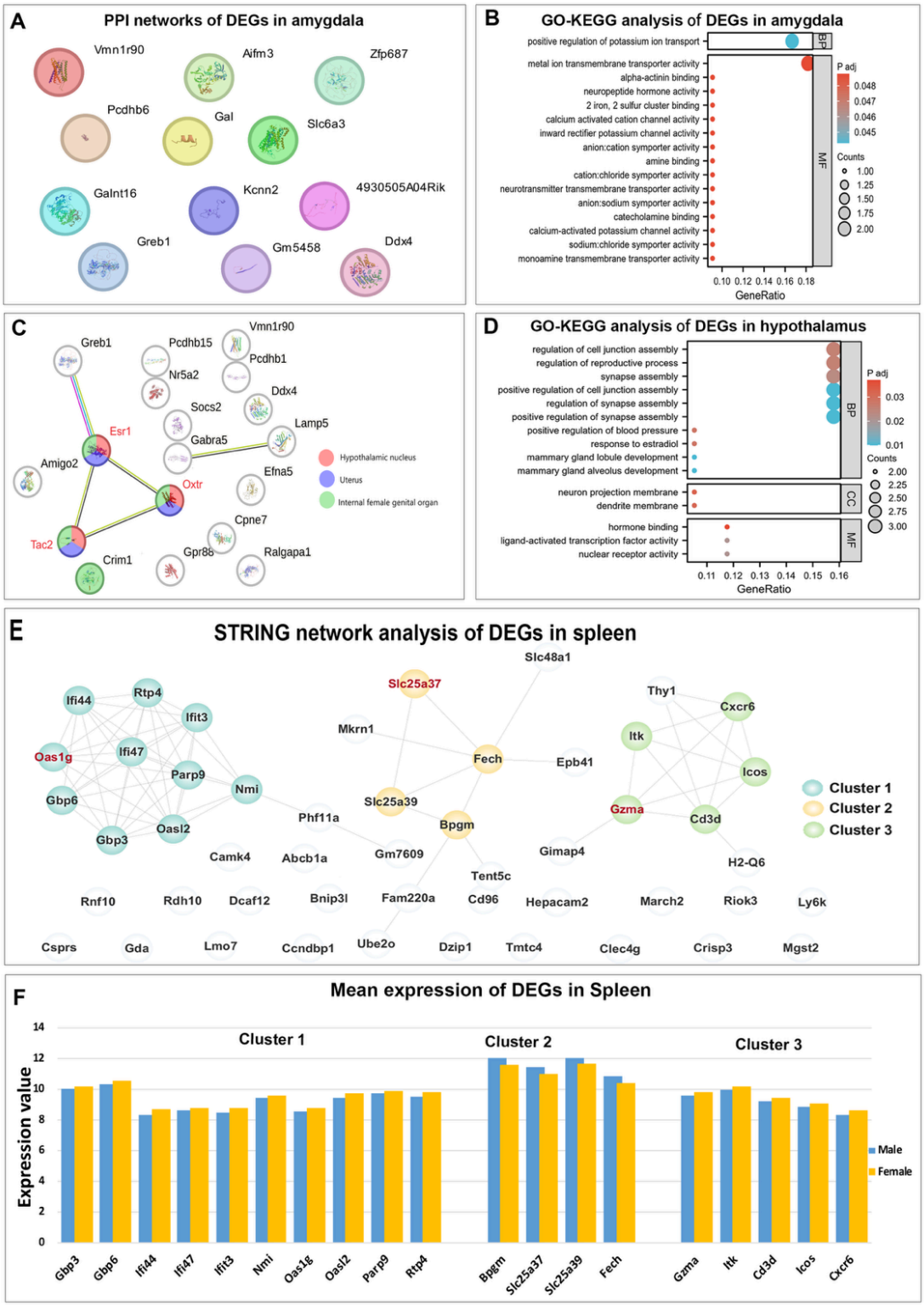


Figure 6

Tissue-specific autosomal DEGs in amygdala, hypothalamus, and spleen. (**A**) Protein–protein interaction analysis of amygdala autosomal DEGs. No strongly connected interaction module was detected. (**B**) GO and KEGG enrichment analysis of amygdala autosomal DEGs. Enriched terms were related mainly to ion binding, transporter activity, receptor activity, channel activity, and potassium ion transport. (**C**) Protein–protein interaction network of hypothalamic autosomal DEGs. Nodes represent DEGs associated with neuroendocrine and reproductive-related functions. (**D**) GO and KEGG enrichment analysis of hypothalamic autosomal DEGs. Enriched terms included hormone signalling, nuclear receptor activity, synaptic organization, reproductive regulation, and mammary gland development. (**E**) Protein–protein interaction network of spleen autosomal DEGs. Three major clusters were identified, related to heme metabolism, mitochondrial iron transport, heme biosynthesis, chemokine-mediated signalling, and adaptive immune response. (**F**) Mean expression patterns of spleen DEG clusters in male and female mice.

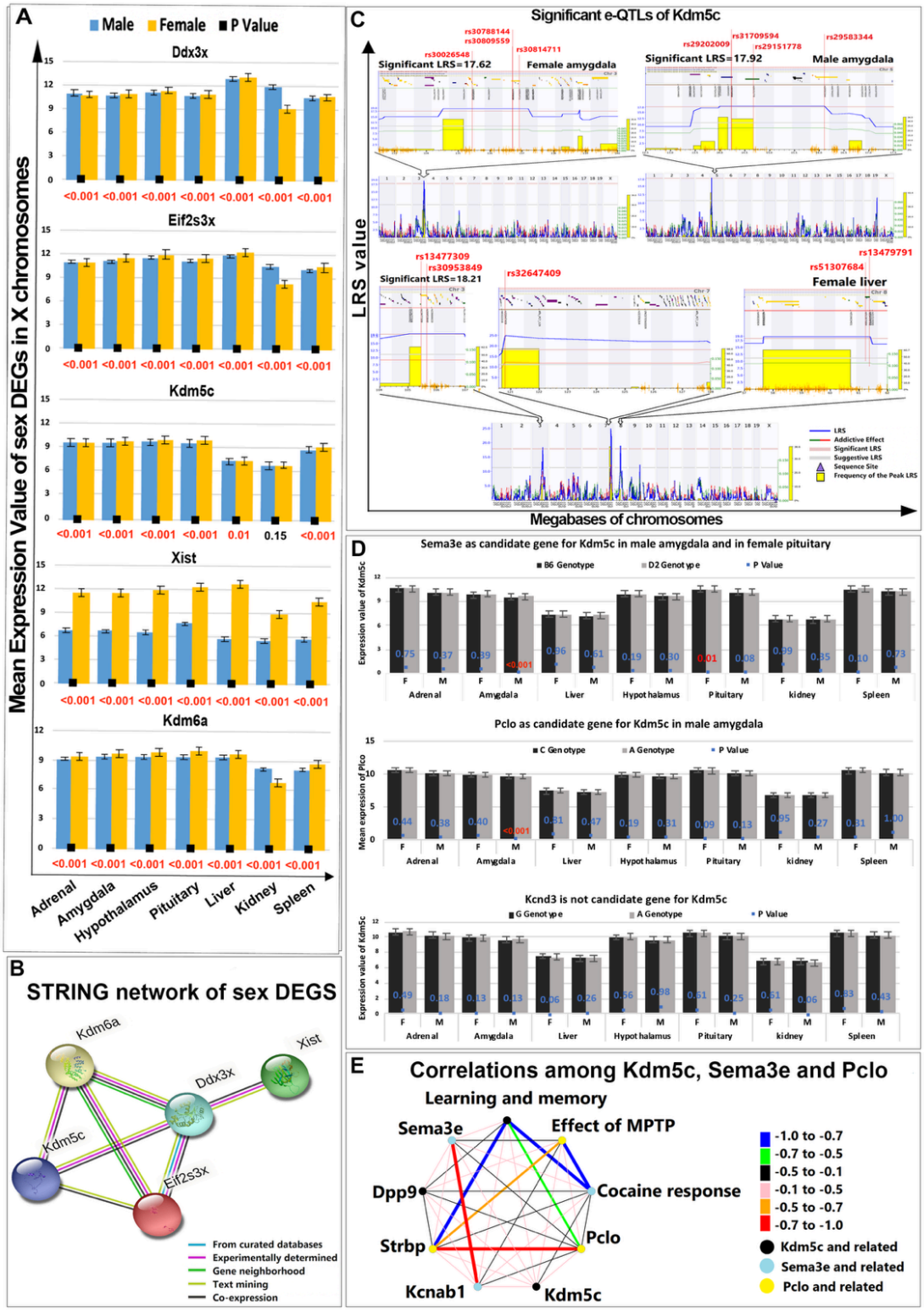


Figure 7

Recurrent X-linked EDEGs and candidate-associated loci. (**A**) Mean expression of recurrent X-linked EDEGs across seven tissues. Genes shown include *Xist*, *Kdm6a*, *Eif2s3x*, *Kdm5c*, and *Ddx3x*. *Xist* showed consistently higher expression in female mice across all analyzed tissues. (**B**) STRING network of recurrent X-linked EDEGs and their first-shell interactors. Nodes represent proteins, and edges represent known or predicted protein–protein associations. (**C**) eQTL analysis of *Kdm5c*in selected tissues and sexes. Loci exceeding GeneNetwork suggestive or significant LRS thresholds are shown. (**D**) Genotype-expression comparisons for candidate-associated loci linked to *Kdm5c* expression. (**E**) Correlation network among *Kdm5c*, candidate-associated genes, and selected GeneNetwork phenotypes. These associations are exploratory and do not establish direct regulatory relationships.

Supplementary Files

This is a list of supplementary files associated with this preprint. Click to download.

- AppendixASupplementarytables.docx
- AppendixB.Supplementaryfigures.docx